國立交通大學

光電工程研究所

碩士論文

設計與製作具應用於 E-Book 之

新型透反式膽固醇液晶顯示器

Design and Fabrication of the Novel

Transflective Cholesteric LCD for

E-Book Application

研究生：黃肇恆

指導教授：謝漢萍 教授

中華民國九十四年六月

設計與製作具應用於 E-Book 之新型透反式膽固醇液晶顯示器

Design and Fabrication of the Novel Transflective Cholesteric LCD for E-Book Application

研 究 生: 黃肇恆　　Student: Chao-Heng Huang
指導教授: 謝漢萍　　Advisor: Dr. Han-Ping D. Shieh

國立交通大學　電機資訊學院
光電工程研究所
碩士論文

A Thesis
Submitted to Institute of Electro-Optical Engineering
College of Electrical Engineering and Computer Science
National Chiao-Tung University
in Partial Fulfillment of the Requirements
for the Degree of Master
In
Electro-Optical Engineering

June 2005
Hsin-Chu, Taiwan, Republic of China.

中華民國九十四年六月

設計與製作具應用於 E-Book 之
新型透反式膽固醇液晶顯示器

研究生：黃肇恆　　指導教授：謝漢萍 教授

國立交通大學光電工程研究所

摘要

傳統膽固醇液晶顯器因其省電的特性非常適合電子書的應用，只需靠環境光源即可閱讀。但有鑑於傳統膽固醇液晶顯示器在這二十年的發展只限於反射模式，所以當環境光源不足時，影象品質變的非常的不清晰。 所以，有人將透反結構應用於膽固醇顯示器，但發現在穿透模式下，暗態會有漏光產生。有鑑於此缺點，我們提出高顯示品質的新型透反式膽固醇液晶顯示器，主要特點是在任何環境光源下皆能顯現出相同的影像顏色，進而提升影像品質。

此新型透反式膽固醇液晶顯示器更特殊的地方是在每一子畫素上分成反射與穿透區域，並在穿透區域上方的玻璃表面加入一光反射影像增強層結構(Image-enhanced reflector)，此結構具有反射穿透光的效果，可以使反射光和穿透光的行進路線近乎相同，使透反式膽固醇液晶顯示器呈現理想的亮態和暗態，在任何環境下，皆可呈現相同色彩的影像，進一步大幅提升顯示影像的品質。

此外我們發現光反射影像增強層結構可以製成薄膜型態故只需貼在傳統反射式液晶顯示器上機板上面，即可升級爲透反式液晶膽固醇顯示器。又，我們亦開發出平版型光反射影像增強層，其出光效率不僅略優於傳統光反射影像增強層且製程簡單，十分便於在 TFT 廠內大量製作。

Design and Fabrication of the Novel Transflective Cholesteric LCD for E-Book Application

Student: Chao-Heng Huang **Advisor: Prof. Han-Ping D Shieh**

Institute of Electro-Optical Engineering
National Chiao Tung University

Abstract

A novel transflective cholesteric liquid crystal display is demonstrated by using cholesteric liquid crystal as a LC layer and an image-enhanced reflector (IER) on the top of the transmissive sub-pixel, providing the similar paths for both reflected and transmitted light, and two circular polarizers laminated on the upper and rear substrates. An extended IER (EIER) is applied to enhance the brightness and CR. Further, to simplify the process, the IER can be fabricated as an IER film laminated on the upper substrate. The results revealed the IER constructed as film structure performed superior than that built internally in the cholesteric cell. As a result, Ch-LCD displays the same image color in any ambience, thus greatly improve the image quality of the transflective cholesteric LCD.

誌謝

首先，我要感謝我的指導教授 謝漢萍老師在這兩年來細心及嚴厲的指導，在邏輯的思考給我很大的幫助及改善，每次在老師嚴格要求完之後，感覺自己都有進步，因有老師不厭其煩的教導，才有繼續進步的空間，也謝謝您讓我在這兩年中參加許多的 Conference 以及有機會在華映合作一年，我從中學習很多，這些經驗對未來在工作及作人都非常有幫助。

也非常感謝實驗室所有成員的相助，謝謝白乙學長在此題目的基礎上奠定良好的成就，同時，也感謝實驗室裡的同學及學長學姐及 Dr. Pani Kumar 在實驗的方法上做指導。

此外，感謝華映的陳司芬處長及華映的工程師:謝謝你们在這一年給我許多技術上的協助，由其是朝棟及建霖和冠群謝謝你们在周末也能夠挺身相助，得以完成實驗。

最後我要感謝我家人的栽培和女友給我心裡上的支持，陪我度過這兩年。

感謝 主耶穌基督，在生活及態度上給我磨練，讓我知道謙卑的重要。

Table of Contents

Figure caption

List of Tables

Chapter 1

Introduction

1.1 Portable Display Technology

The portable displays, such as E-Books and E-papers, have received tremendous attention recently because these displays are characteristic of light weight and large of information content. Portable displays offer two critical advantages over conventional printed paper. First, E-book display is as portable as a paperback and can hold a small library's worth of information. Second, as the internet hyper-growth continues, the electronic publishing is an emerging market. People can download a novel spending only a few dollors, which is less expensive than buying paper-printed books. Therefore, with the assistance of E-books, people are able to carry a volume of favorite publications like books, textbooks, news, newspaper, report, periodicals, and all other related information without any difficulty. Thus, E-book is expected to replace paper as it combines the features of paper and of modern, portable, wireless electronic devices as shown in Fig. 1.1.

Fig. 1.1 Photograph of E-book with paper-like readability

Since readers desire to read portable displays like a real book, a good performance including paper-like (Black and white) readability and excellent readability in any ambient light is of great importance. Low power consumption and low cost are the second concerned issues. Full-color capability is the third essential issue. Comfortable holding and easy carrying may be other important requirements. Thus, the target for portable displays performance standards is achieving that of printed paper, in terms of brightness, contrast ratio, and legibility.

In order to meet all the basic requirements mentioned above, several e-book display technology have been actively pursed, including liquid crystal display, organic light emitting display and particle displays. In the category of liquid crystal display, the Cholesteric Liquid Crystal Display (Ch-LCD) is, so far, one of the best solutions to E-book displays application. Tab 1.1 [1] shows calculated battery life of a VGA, 6.3-inch diagonal full color display in terms of the battery (5.4Watt-hours) lifetime or operating time between battery recharges for different display technologies.

Tab. 1.1 Lifetime time between battery recharges for different display technologies

Display Technologies	Time Between Recharges for Various Average Reading Times		
	1 min/page	2 min/page	5 min/page
Refreshed type display with backlight such as an STN or Active Matrix TN.	2hrs	2hrs	2hrs
Refreshed type reflective display with smart electronics.	18hrs	18hrs	18hrs
Bistable reflective Cholesteric display passive matrix addressing.	270hrs	540hrs	1350hrs
Bistable reflective Cholesteric display active matrix addressing 50% pixel change.	640hrs	1280hrs	3200hrs

1.2 Advantages and Issues of Bistable Reflective Cholesteric Displays

Bistable reflective cholesteric displays technologies [2][3] are of increasing interest as the industry looks to develop product with low power consumption and high brightness for portable display applications. The main advantage of reflective cholesteric device is that it does not require any polarizer (thus high brightness) or a

backlight (for daytime operation) and is bistable (do not require continuous image updating) with excellent viewing angles, good contrast. Thus, reflective Ch-LCDs are uniquely suited for portable devices (e-books).

However, since the reflective Ch-LCDs use the ambient light to display images, the display luminance particularly depends on the surrounding environments, and it always loses its visibility under dark ambient. Further, it is hard to control the purity of the ambient light, therefore, such a reflective Ch-LCD do not provide sufficiently high quality in terms of brightness, contrast and color saturation. Accordingly, further improvement in brightness and contrast for portable devices is demanded. In order to overcome the issues of reflective Ch-LCD, a configuration which realizes both the transmissive and reflective modes display in one liquid crystal device has been disclosed and named transflective type LCDs, as shown in Fig. 1.2. Thus, a prime importance of transflective modes operation is required for the good legibility in any ambient condition. However, such a transflective type structure is not able to apply in reflective cholesteric displays. In the following section the operational principle of the conventional transflective Ch-LCD as well as its concerned issues will be illustrated.

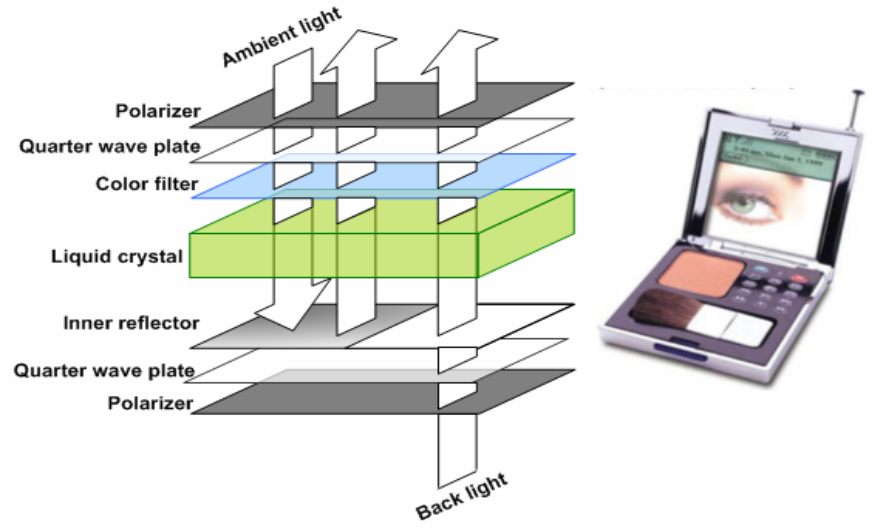

Fig. 1.2 Transflective type LCDs

1.3. Conventional Transflective Cholesteric LCD

The liquid crystal displays using both the transmitted light and reflected light are generally referred to transflective LCDs, which can be used under the circumstance where the ambient light is weak while maintaining the advantages of the reflective Ch-LCDs. Following the approaches and characteristics of different types of transflective Ch-LCD will be introduced.

1.3.1 Transflective Cholesteric LCD with sub-pixel Structure

In a transflective STN or TFT LCD, each pixel is divided into transmissive and reflective sub-pixels. Following the operational principle of Ch-LCD is desecrated. To enable a Ch-LCD to be useable in any ambience conditions, each pixel is divided into transmissive and reflective sub-pixels, as shown in Fig.1.3. The operation principle of a reflective region is shown in left-part of Figs. 1-3. (a) and (b). In a planar state, as an unpolarized light is incident into a left-hand cholesteric LC layer. Due to Bragg condition [5], the left-hand circularly polarized light within the bandwidth is reflected and the transmitted right-hand circularly polarized light is absorbed by the absorption layer. As a result, the bright state is achieved. In a focal conic state, the incident light passing through the LC layer is absorbed by the absorption layer, resulted in a dark state.

The operation principle in transmissive region is shown in the right part of Figs. 1-3. (a) and (b). In a planar texture, an unpolarized backlight is incident into cholesteric LC layer. The left-hand circularly polarized light within the bandwidth is reflected and the transmitted right-hand circularly polarized light is passed through the cholesteric LC layer. As a result, the bright state is achieved. In a focal conic state, the backlight passing through the LC layer causes a light leakage, resulting in the bright state. Thus, both reflective and transmissive sub-pixels display bright state, but

lack of dark state. As a result, such a split pixel approach does not apply to the cholesteric display.

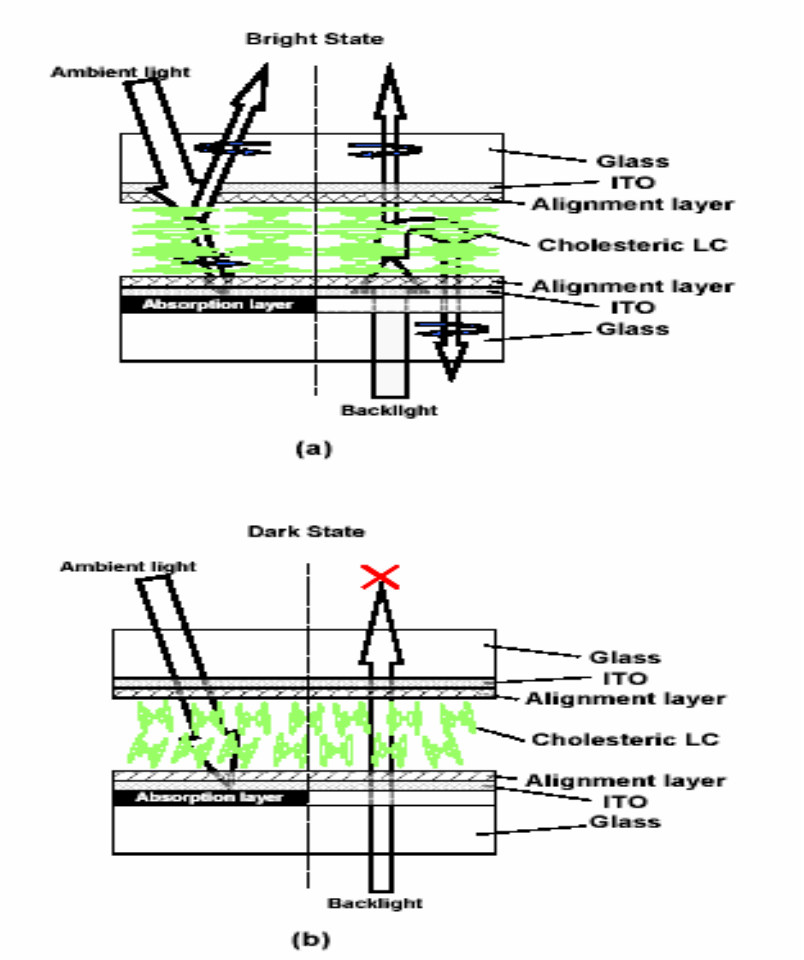

Fig. 1.3 Operation principle of reflective/transmissive cholesteric display. (a) Planar and (b) focal conic state.

1.3.2 Transflective Ch-LCD with Front Lighting

Since this type of transflective structure with sub-pixel structure cannot apply to Ch-LCD, another method called transflective Ch-LCDs with front lighting (FL) approach was proposed [6]. Following the approach and characteristic of this type transflective Ch-LCD will be introduced. Since purely reflective displays have poor performance in low ambient lighting conditions, auxiliary lighting is required. Generally, front or edge lighting is required to read information contents for dark ambience condition. Front lighting is usually done with the help of a light steering

plate that is placed on top of the display.[] Edge lighting employs illumination sources at the edges of the display.

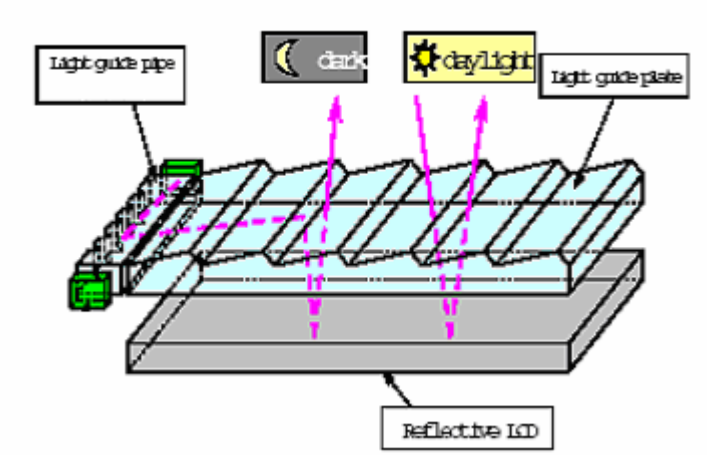

Fig. 1.4 Schematic of front lighting system

Fig.1.4 shows the basic construction of front lighting (FL) situated on LCD. The image quality of displays maintained by FL is required not only when LED switches on in the dark place but also when it usually switches off under daylight condition. Thus, FL is designed as possible as transparent when switch is off in bright ambience condition. When switch is on, the refractive light bent by the prismatic array is incident perpendicular to the reflective LCD. However, both scenarios have drawbacks. The edge lighting tends to be less uniform whereas the front light steering plate usually distorts the image. Hence, both scenarios cannot be employed effectively on cholesteric displays.

1.3.3 Birefringent Color Reflective LCD Using Broadband Cholesteric Reflectors

Philips also proposed a method relating to the transflective Ch-LCD [7]. The device structures are shown in Fig. 1.5. The main idea of this type of transflective Ch-LCD is that their cholesteric layer is used as a transmissive reflector, here, the transflective display is obtained without sacrificing the brightness of the reflective or the transmissive mode. Nevertheless, when the display is operated in the transmissive mode, a

complementary color is obtained. In a monochromatic Ch-LCD application, this type of device is sufficient. When applied in the full color Ch-LCD, however, displaying the complementary color in different modes will lead to a serious issue.

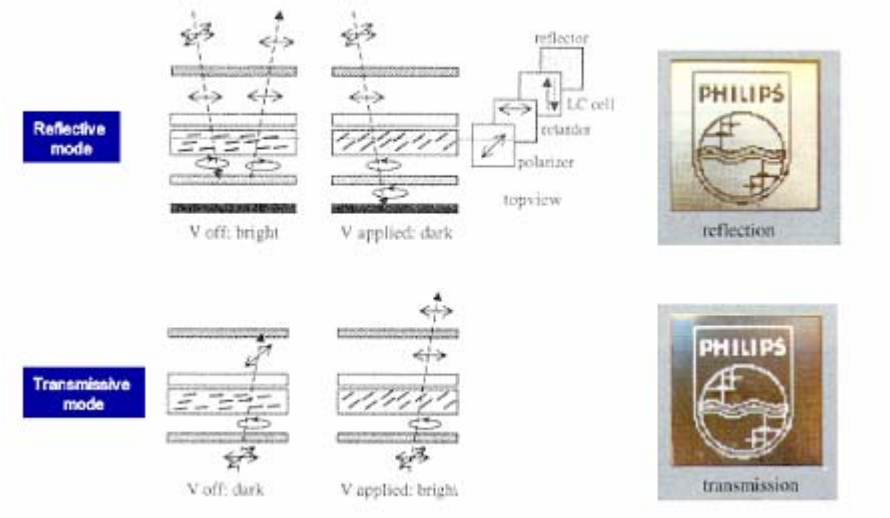

Fig. 1.5 Principle of switching between white and black states in the reflective mode, for LC cells and retarder combined with a cholesteric reflector.

1.4 Motivation and Objective of this Thesis

The conventional reflective Ch-LCDs are actively studied because of their advantages and characteristic such as high brightness, low power consumption, bistable property, and simple manufacturing process . Due to its bistability, the driving voltage is required only when refreshing the screen, resulting in consuming less power than the general reflective STN or TFT displays. An ordinary people may take 2-3 minutes to complete reading one page. Thus, this power-saving feature enables Ch-LCD a strong contender for e-papers or e-books.

Conventional reflective Ch-LCDs utilize the ambient light to display the information contents. In a dark ambience, however, the displays are not readable. Further, the application of transflective mode enables STN and TFT-LCDs to be readable in dark ambience, nevertheless, Ch-LCDs are still not applicable for such

transflective structure due to lack of dark state in transmissive region. Therefore, for cholesteric-display technology to be widely competitive in portable display application with existing technologies, such as reflective STN and TFT displays, and other emerging technologies, such as particle-based displays (EINK or Mircocup) and organic light-emitting devices(OLED's), the next generation of cholesteric displays will need to have features like portability, low-power consumption, full-color capability, ruggedness, high brightness and transflective dual-mode operation.

Since purely-reflective Ch-LCD has poor performance in low lighting condition, in order to overcome these problems, we present a newly developed transflective Ch-LCD with same-image color display by building an image-enhanced reflector (IER) [8] and Extended IER (EIER) on the top of transmissive region along with the function of circular polarizers. This novel display can be used both in a fully reflective mode as well as a fully transmissive mode, which greatly enhances the usefulness of Ch-LCD by enabling its use in low ambient lighting conditions. The adequate legibility under both bright and dark scenes was anticipated.

IER/EIER reflectors were designed between the gaps of adjacent pixel in place of the black matrix for high area utilization and results in high aperture ratio. Both reflectors are to build in the path of the backlight to reflect the transmitted light to the reflective region. Thus, the backlight and ambient light follow the similar paths, and leads to same optical efficiency and color saturation. Also, EIER reflectors offer additional functions including luminance and contrast enhancement.

1.5 Organization of this thesis

The thesis is organized as following: the principles and the features of the new transflective Ch-LCD will be presented in Chapter 2. The mode of operation will be discussed. In Chapter 3, the optical simulation software will be used to simulate the light utilization efficiency and obtain an optimized structure for practical utilization.

The simulated results including luminance, contrast and light distribution were used to verify and optimize our design. In Chapter 4, the fabrication technologies to realize our new transflective Ch-LCDs are summarized. The measurement equipments will be illustrated. In Chapter 5, the fabricated transflective Ch-LCD device with IER/EIER structure and circular polarizers will be demonstrated. Further, the measurement results including optical and electrical performances will be evaluated. The summary of the dissertation and the future works are given in Chapter 6.

Chapter 2

Principle

2.1 Introduction

Due to the technical challenge for the traditional reflective Ch-LCD, we propose a novel transflective Ch-LCD by using an image enhanced reflector (IER), an extended IER (EIER) and two opposite handedness circular polarizers to provide the bright state and dark sate in reflective and transmissive modes. Fig. 2.1 illustrates the configuration of the transflective bistable cholesteric display. The liquid crystal display device includes two glass substrates with a single cell gap liquid crystal layer in both reflective and transmissive sub-pixels interposed. Thus, in this novel transflective Ch-LCD, each pixel is divided into reflective and transmissive regions, which is the first time demonstrated in the Ch-LCD devices. In transmissive region, an image enhanced reflector (IER) and extended IER (EIER) are in position to reflect the backlight into reflective pixels, providing the similar path for both reflective and transmissive light. The EIER is used for enhancing the brightness and contrast. There is a backlight source at the back of the display, followed by the Ch-LCD sandwiched by two circular polarizers. With the function of the circular polarizers, the bright state and dark state of reflective and transmissive modes for Ch-LCD are achieved. The handedness of the emergent circular light depends on whether the transmission axis of the linear polarizer is at +45˚ or -45˚ to the fast axis of the retarder. Assume the cholesteric layer is left handed, so that it reflects the left-hand (L) circularly polarized light and transmits the right-hand (R) circularly polarized part. Thus, the upper circular polarizer is left-circular polarizer (LCP) and rear circular polarizer is right-circular polarizer (RCP). As a result, a novel transflective Ch-LCD was realized by using cholesteric liquid crystal as a LC layer and IER/EIER on the top of the transmissive sub-pixel, providing the similar paths for both reflected and transmitted light, and two circular polarizers laminated on the upper and rear substrates.

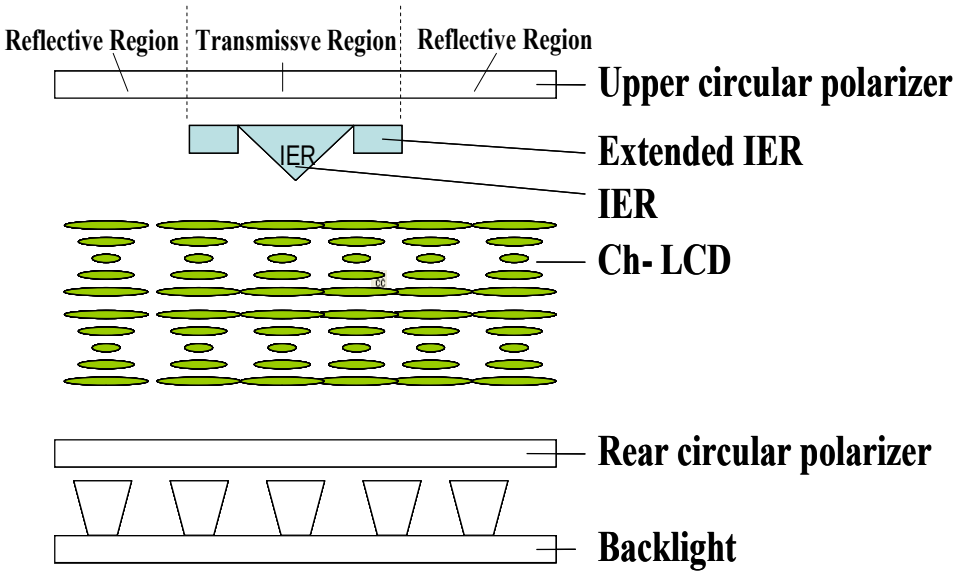

Fig. 2.1 The basic configuration of the transflective Ch-LCD with IER/EIER structures and circular polarizers

2.2 Optical Properties of Cholesteric Liquid Crystal

The cholesteric (Ch) phase is a liquid crystal phase exhibited by chiral molecules or mixtures containing chiral components. The state of the cholesteric liquid crystal is characterized by the direction of the helical axis as shown in Fig. 2.2. In the planar texture, the helical axis [9] is perpendicular to the cell surface as shown in Fig. 2.2(a). The material reflects light centered at wavelength given by $\lambda_0=nP_0$[10][11], where n is the average refractive index. If λ_0 is in the visible light region, the cell has a bright colored appearance. In the focal conic texture, the helical axis is more or less parallel to the cell surface, as shown in Fig. 2.2(b)[12]. When the pitch is short, the cholesteric liquid crystal can be regarded as a layered structure, which is a multiple domain structure, and the material is scattering. When the applied field is larger than a critical field *Ec*, the helical structure is unwound with the liquid crystal director aligned in the cell normal direction as shown in Fig. 2.2(c). This texture is called the homeotropic

texture. With the appropriate surface anchoring condition or dispersed polymer [12], both the planar texture and the focal conic texture can be stable at zero field.

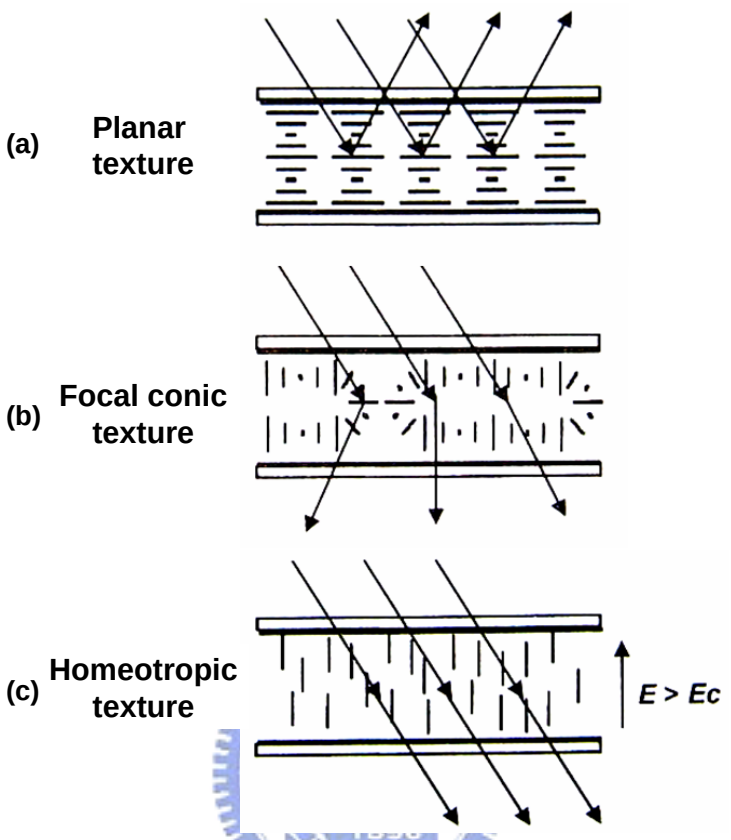

Fig. 2.2 The structure of the cholesteric textures: (a) planar, (b) focal conic, and (c) homeotropic texture.

The operation principles of Ch-LCDs are illustrated in Fig. 2.3. In the voltage-off state, the planar texture reflects brilliant colored light if the Bragg reflection condition ($\lambda_0 = nP_0$) is satisfied. The bandwidth $\Delta\lambda$ of the reflected light is equal to $\Delta n\, P_0$; here Δn is the birefringence of the LC. For a display in the visible region, λ_0 = 550nm, n =1.6 and $\Delta n = 0.2$, the pitch length P_0 is 344nm and the bandwidth $\Delta\lambda$ is 70nm. In a helical structure, circularly polarized light with the same handedness as the helical structure is reflected strongly because of constructive interference of the reflected. While circularly polarized light with the opposite handedness to the helical structure is not reflected because of the destructive interference. An incident unpolarized light

is decomposed into right and left circular polarized components with one component reflected and the other transmitted. The transmitted light is absorbed by the black paint coated over the rear substrate, as shown Fig. 2.3(a). In a voltage-on state (Fig. 2.3(b)), the periodic helical structures are changed to focal conic. As a result, the Bragg reflection is interrupted. The incoming light is absorbed by the dark paint and a dark state is obtained.

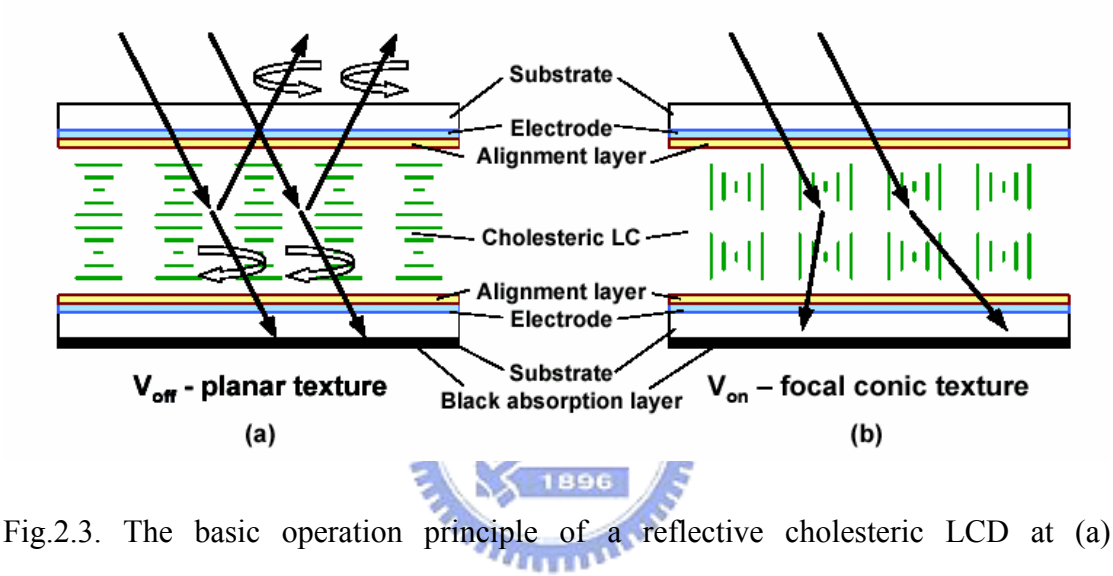

Fig.2.3. The basic operation principle of a reflective cholesteric LCD at (a) Voltage-off and (b) Voltage-on state.

Although cholesteric liquid crystals are only bi-stable, they exhibit gray scale memory states because of their multi-domain [13][14]structure. Starting from the imperfect planar texture, some domains can be switched to the focal conic texture at lower voltages than other domains. Once a domain has been switched to the focal conic texture, it remains there even after the applied voltage is turned off. Fig. 2.4 shows microphotographs of the gray scale states of a cholesteric display. From right to left, the states are achieved by applying voltage pulses with increasing amplitude, and the reflectance decreases. The domain size is around 10 μm and the domain structure

cannot be observed by the naked eye. The typical pixel size for Ch-LCD is about 200μm. It is misleading to call the Ch-LCD multi-stable. A cholesteric domain has only two stable states at zero field: it is either in the planar texture or in the focal conic texture. In a Ch-LCD, it is observed that the domains in the planar texture have the same optical properties, independent of the states of other domains.

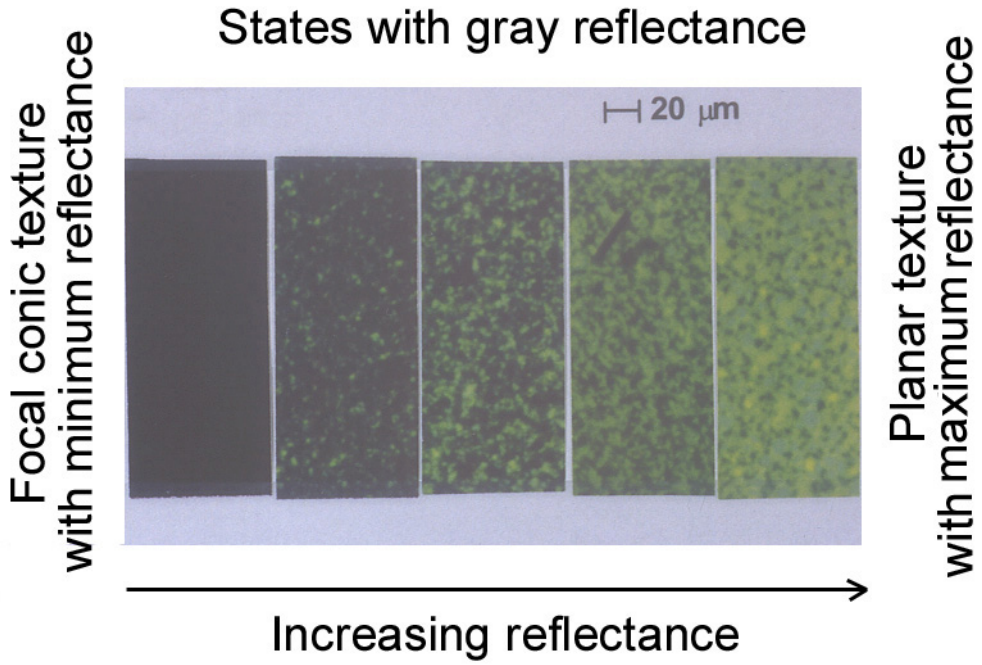

Fig.2.4 The microphotographs of the gray scale states of the cholesteric display [15]

An important feature of the Ch-LCD is that the reflected light is already colored. Therefore, a mono-color display without using color filters can be easily achieved. In addition, no polarizer is needed. Thus, the brightness of a Ch-LCD is higher than a reflective color display employing one polarizer. To achieve multiple colors, three monochrome R, G, and B panels can be stacked [16][17] together. A potential problem of the stacked approach is parallax, i.e. the incident light and reflected light pass through different pixels. Parallax leads to color mixing which becomes a serious issue

for high-resolution LCD. In order to decrease parallax, thin substrate, preferably substrates with conducting coating on both sides, should be used to decrease the spacing between the liquid crystal layers. The measured reflection spectra of three-layer cholesteric display is shown in Fig. 2.5.[18] Without using a polarizer, the reflectance is around 30% ~ 35%, and its contrast ratio is in the range of 5-10 within 60^{o} viewing cone.

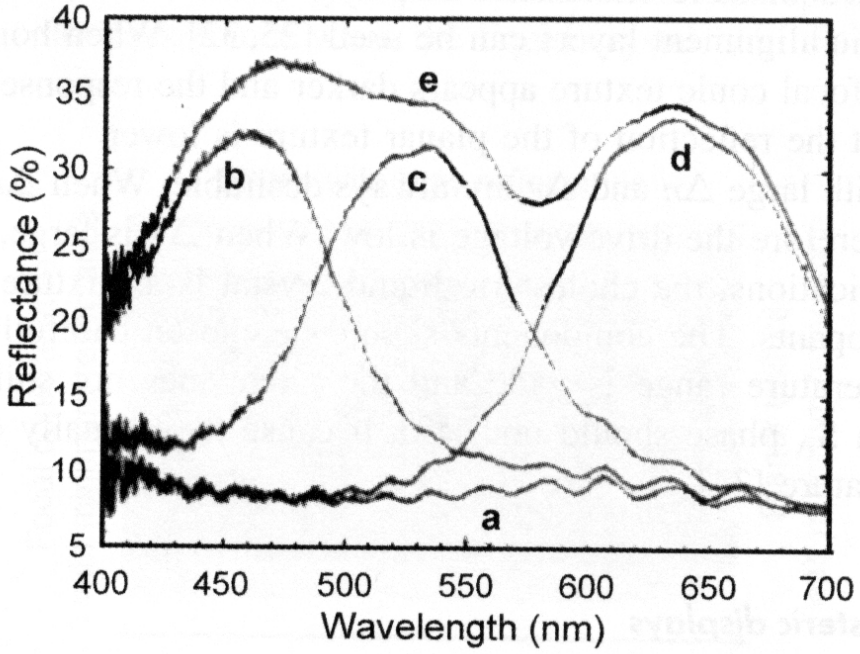

Fig.2.5. Reflection spectra of the stacked multiple color cholesteric display. Curve a: all off, curve b: blue on, curve c: green on, curve d: red on, curve e: all on[19].

However, the stacking method is still too complex to fabricate a full color Ch-LCD. Additionally, conventional cholesteric LCD cannot display same image color in reflective and transmissive modes. Therefore, it cannot be used in different ambiences, thus, restricting the applications of Ch-LCDs.

2.3 Features of Full-color Transflective Cholesteric LCD

In order to realize the principle of the transflective Ch-LCD, this section is devoted to introduce some properties and advantages of this novel transflective structure.

2.3.1 Transflective Cholesteric LCD

Assume the cholesteric layer is left handed, so that it reflects the left-hand (L) circularly polarized light and transmits the right-hand (R) circularly polarized part. In the reflective mode, the backlight is off and we describe two cases of light output. In the planar state, the ambient light is incident to reflective pixels and transformed into L light by the left circular polarizer. Since the cholesteric layer is left handed, the L light is reflected within the reflection band of the cholesteric. As the result, the bright state is obtained, as shown in left part of Fig. 2.6. In the focal conic state, the L light is transmitted by the LC-layer and is absorbed by the right circular polarizer. As a result, the dark state is obtained, as shown in right part of Fig. 2.6

In the transmissive mode, the backlight is on and we describe two cases of light output. In the planar state, the backlight is incident on the transmissive regions and transformed into R light by the right circular polarizer. On the transmission channel, the R light is transmitted to impinge onto the IER. Upon the reflection, the R light becomes L light and is reflected by cholesteric LC layer to the viewer. Again, the bright state is achieved, as shown in left part of Fig. 2.7(a). On the other hand, when the voltage is applied the LC is reoriented to the focal conic state. The backlight initially converted to R light is transmitted by the LC-layer and becomes L light upon the reflection on IER. The L light is eventually absorbed by the right circular polarizer. Hence, the dark state is achieved, as shown in right part of Fig. 2.7(a). Furthermore, a portion of backlight, which is initially converted to R light and does not impinge onto the IER structure, will eventually absorbed by the left circular polarizer and hence the dark state is obtained, as shown in right part of Fig, 2.7(a). Hence, the same bright state and dark state for both reflective and transmissive channels is achieved since an IER structure on the top of transmission channel provides the similar path for both reflective and transmissive light. Thus, the complementary color will not appear as the transmissive mode is on. This is essential for full-color Ch-LCD applications since the

backlight is needed to turn on for obtaining the same color saturation in the not-to-dark ambience.

The Extended IER (EIER) structure is applied to enhance the luminance and contrast. In the planar texture, the oblique backlight is transformed into R light by the rear circular polarizer. The oblique R light becomes L light upon the reflection on the EIER. The L light is reflected by cholesteric LC layer to the viewer, thus the brightness is enhanced by using the oblique light efficiently, as shown in left part of Fig. 2.7(b). In the focal conic state, the oblique backlight initially converted to R light is transmitted by the LC-layer and becomes L light upon the reflection on EIER. The reflected L light is then absorbed by right circular polarizer. Thus, CR is enhanced by blocking the oblique light for dark state, as shown in right part of Fig. 2.7(b). Further, the similar path for both reflective and transmissive light is also achieved by the function of EIER. As a result, an IER as well as EIER on the top of the transmissive region provide the similar paths for both transmissive and reflective light. The two regions can always display same image color in any ambience, thus to greatly improve the image quality of the transflective cholesteric liquid crystal display in both monochromatic and even full-color capability applications.

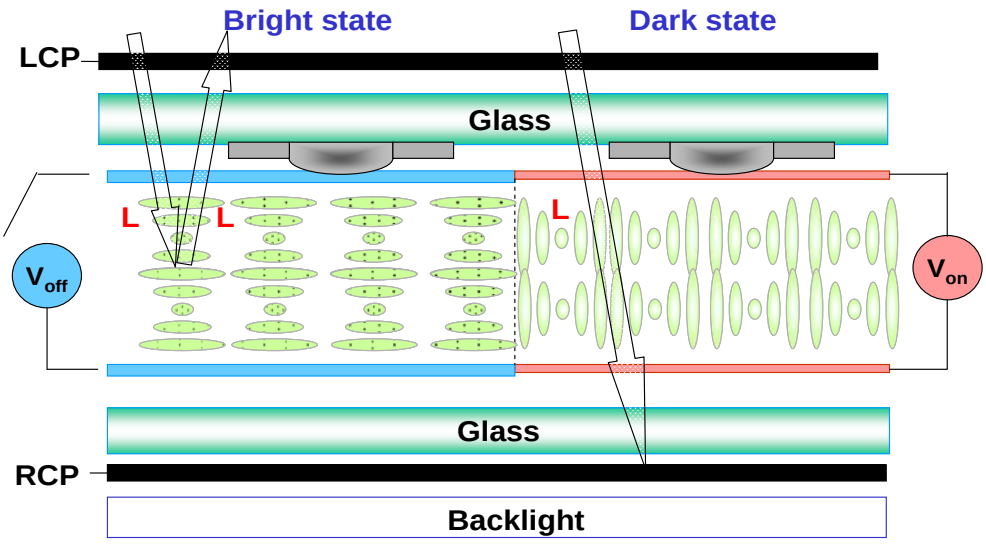

Fig. 2.6 Schematics of the reflective mode for the proposed transflective Ch-LCD

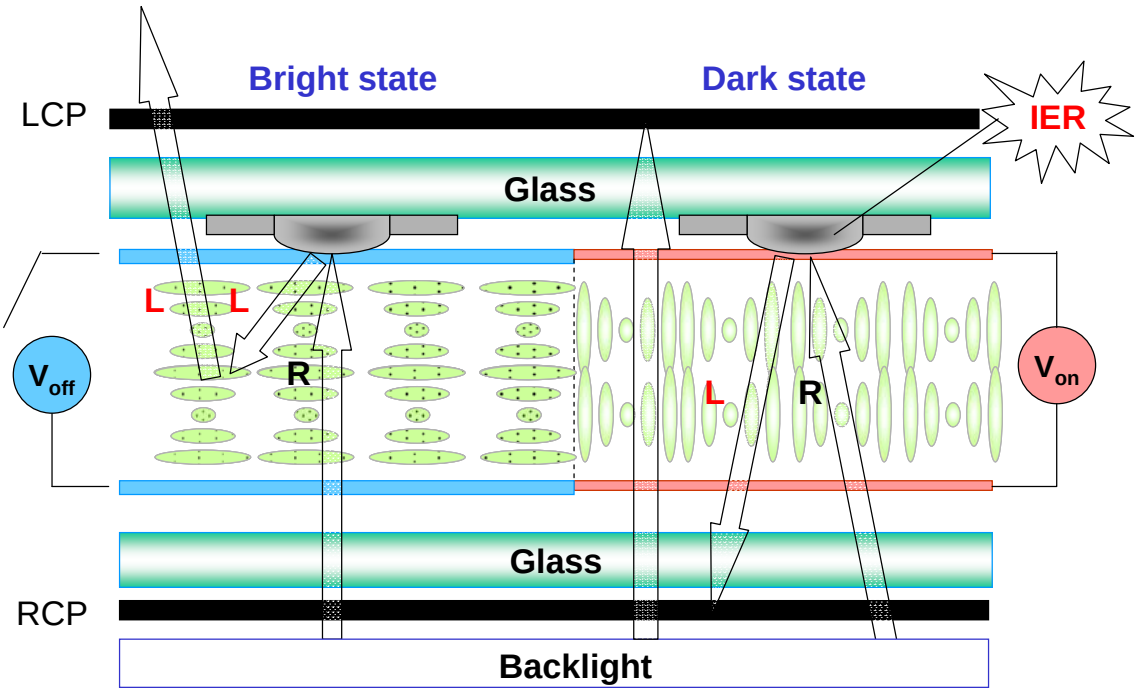

(a)

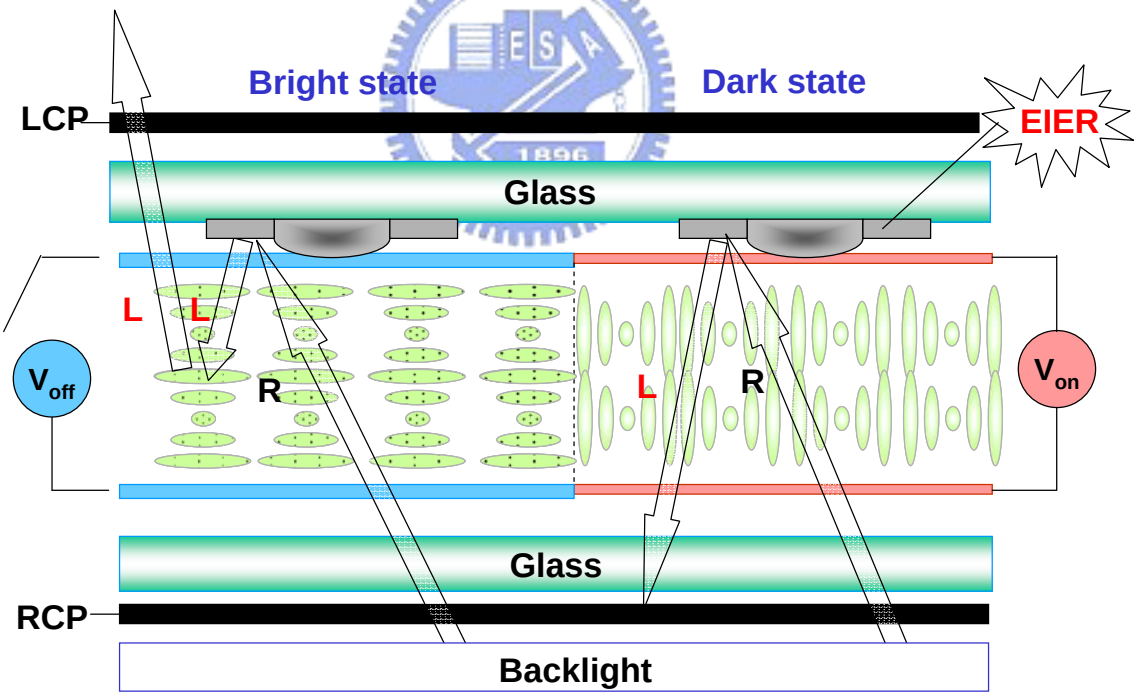

(b)

Fig. 2.7 Schematics of the proposed transflective Ch-LCD for transmissive mode with (a) IER and (b) EIER structure

2.3.2 High area utilization and high aperture ratio

The IER and EIER structures were built between the upper glass and ITO transparent electrode, as shown in Fig. 2.8. Accordingly, from the top-view of each of the plurality of pixel areas as shown in Fig, the IER and EIER were designed between the gaps of adjacent pixel in place of the black matrix for transmissive mode. Therefore, the area utilization or aperture ratio in our deign is reached to almost 100%.

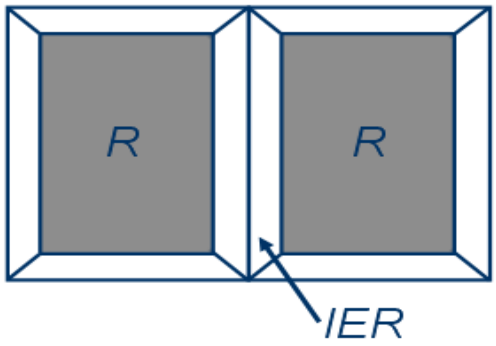

Fig. 2.8 Top view of side IER structure

2.4 Summary

The optical properties of cholesteric textures were illustrated. The proposed configuration and operational principle were discussed and demonstrated. The IER/EIER were built on the location of black matrix, thus to obtain nearly 100 % aperture ratio. Based on Bragg reflection of cholesteric LC in the planar texture, with the IER/EIER as well as functions circular polarizers, the bright states of both transmissive and reflective modes were obtained. Moreover, based on the scattering effect of cholesteric LC in the focal conic texture, with the IER/EIER as well as functions circular polarizers, the dark states of both transmissive and reflective mode were achieved. Thus, a novel transflective Ch-LCD was realized by using cholesteric liquid crystal as an LC layer and IER/EIER on the top of the transmissive sub-pixel, providing the similar paths for both reflected and transmitted light, and two circular polarizers laminated on the upper and rear substrates. As a result, the proposed transflective Ch-LCD were applicable to both monochromatic as well full-color devices with same image color in any ambience.

Chapter 3

Simulated Results and Discussions

3.1 Introduction

Based on the principle described in charter 2, we begin to establish a simulation model used to characterize the features of the transflective Ch-LCD with IER/EIER structures and circular polarizers. The optical analysis simulator TracePro was selected to perform the simulation on the properties of luminance and contrast of transmissive mode in the proposed transflective Ch-LCD. First, the IER/EIER structures were simulated and optimized. Then, the performance of transflective Ch-LCD was improved by the optimization of overcoat layer. Finally, a novel transflective Ch-LCD with good luminance and high contrast as well as simple fabrication process was realized with IER/EIER and circular polarizers.

3.2 Simulation software

The optical simulator TracePro, developed by Lambda Research Corporation, was used to design the optimized transflective Ch-LCD and simulate its transmissive light luminance and contrast.

3.2.1 TracePro

TracePro uses Monte Carlo ray tracing to compute optical flux as it propagates through a model. TracePro accounts for absorption, specular reflection and refraction, scattering and aperture diffraction of light. Results can be examined in spatial Irradiance plots, angular radiance plots, contour maps, Candela plots, or ray histories

in tabular form.

3.3 Optimized IER/EIER structures and overcoat layer

As mentioned in chapter 2, an IER bump and EIER flat structures employed between the upper glass and ITO transparent electrode were used to reflect the transmitted light to follow the ambient light with similar paths. Therefore, in this section, TracePro is used to perform the simulation. The transflective Ch-LCD with IER/EIER and circular polarizers will be designed and optimized.

3.3.1 Simulation Configuration

The simulation configuration including two circular polarizers with opposite polarity, bump IER structures, flat EIER structures, and reflectors symbolized cholesteric liquid crystal layer, $\lambda/2$ retardation film, and light source is shown in Fig. 3.1. The IER/EIER structures were built between adjacent sub-pixels with merits of high area utilization and high aperture ratio, which is named as the "side IER structure", as shown in Fig. 2.8.

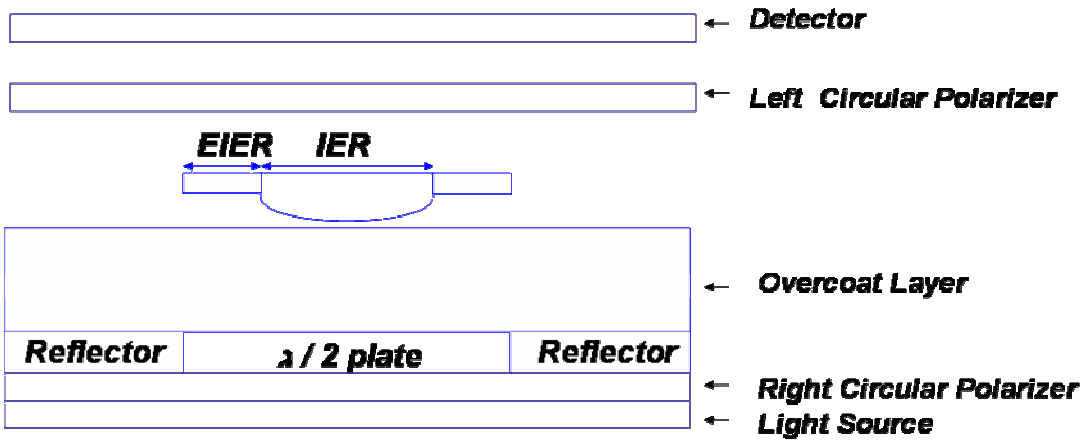

Fig. 3.1 Schematic drawing of the simulation configuration

Since TracePro does not provide with the cholesteric liquid crystal, we use reflectors along with $\lambda/2$ film to symbolize the cholesteric-like Bragg reflectors.

Beside, the distribution of the back light was designed similarly to those of the commercial product where the Brightness Enhancement Film (BEF) was incorporated. BEF is a micro-replicated enhancement film that utilized refraction and reflection of a prismatic structure to increase the light efficiency. Therefore, in the simulation configuration, the backlight was simulated as a crossed BEF distribution, as shown in Fig. 3.2

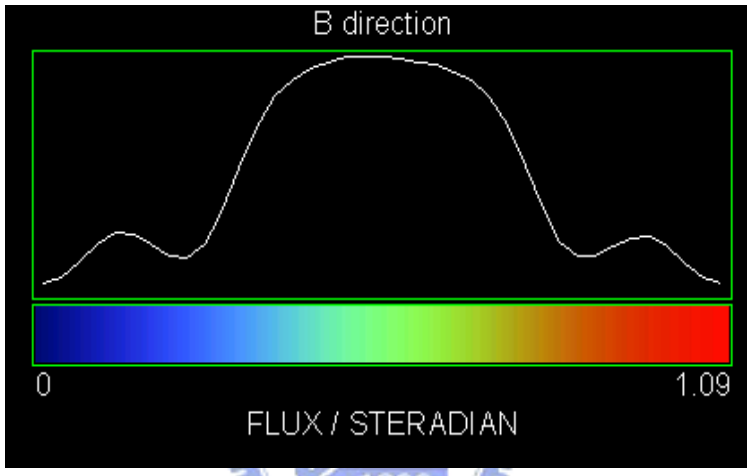

Fig. 3.2 Simulated backlight with BEF distribution

3.3.2 Simulated results

The IER structure was designed as a bump-shaped structure, since this shape is able to reflect the transmitted light to the adjacent sub-pixels in a uniform distribution fashion. We optimized the transflective Ch-LCD by varying the IER/EIER widths and the overcoat thickness, distance between the IER and cholesteric-like reflectors, as shown in Fig. 3.3.

The simulation parameters are shown in Tab. 3.1. The portable displays were usually observed at the polar angle ranging from -30° to 30°. Besides, the tilt angle of IER was essential for the light distribution. Thus, according to the reflection theory, the angle of IER was designed 15° to obtain this specific light distribution as well as

to make the transmitted and reflective components followed the similar path.

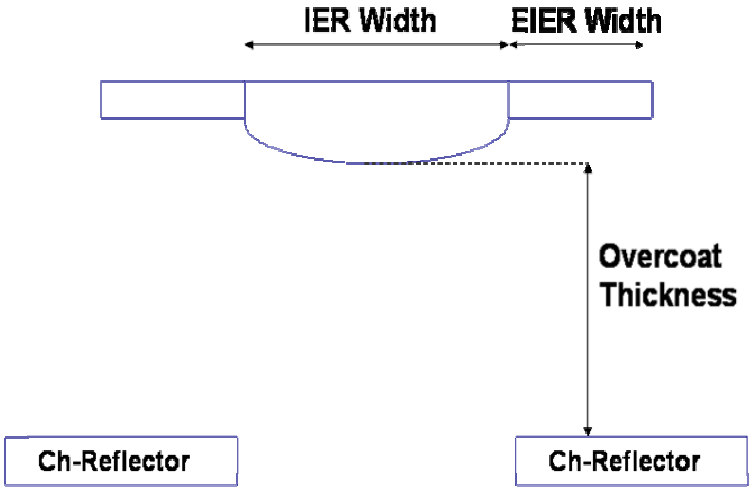

Fig. 3.3 Variations of the simulation for optimizing the IER structure

Tab. 3.1 Simulation parameters

Parameters	
Pixel Size (μm)	210 * 210
Thickness of the Glass (μm)	550
Angle of the IER (degree)	15
Rays number	10^8

3.3.2.1 EIER optimization

The IER width was first fixed to 14μm and the overcoat thickness to 30μm, the width of EIER was optimized by varying its width from 0 to 9 μm. The results, as shown in Tab. 3.2., reveal that the light distribution is not affected by the EIER width, because the peak light intensity is distributed at around ±30° no matter how EIER changes. This viewing angle distribution is satisfied with the requirements for the portable display application, as readers usually observe portable devices at the

tilt-angle ranging from 0° to 30°.

On the other hand, the transmissive luminance efficiency rises gradually as the EIER width increased continuously. Eventually, the transmissive light luminance saturated about 8.7 %, as shown in Fig. 3.5. Further, the transmissive contrast decreases rapidly as the EIER width increased gradually. The high transmissive contrast was achieved when EIER width is larger than 3 μm. Further, the results demonstrated that the transmissive light luminance was increased from 7 % to 9 % when the additional EIER structure was included with the IER structure. Besides, the transmissive contrast was decreased from 10% to 0.1% as the EIER width is increased to 3 μm. Hence, the EIER width of 3 μm was selected to enhance the luminance and contrast in the transmissive mode of the proposed transflective Ch-LCD.

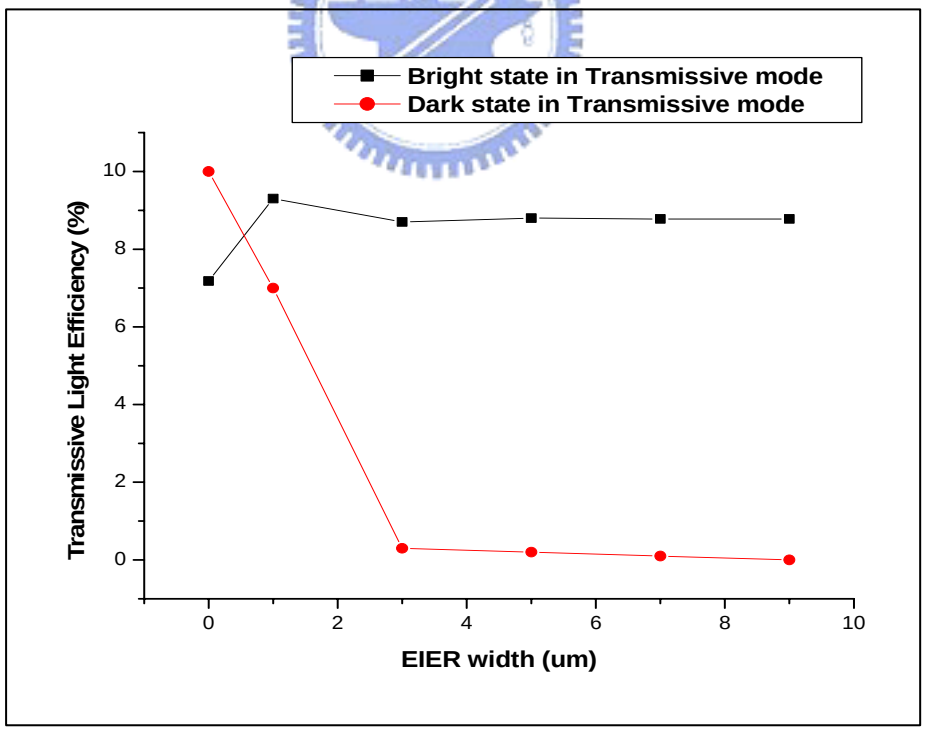

Fig. 3.4 Transmissive light efficiency in bright and dark states with various EIER widths

Tab. 3.2 Transmissive light efficiency with various EIER width

EIER Width (μ m)		0	1	3	5	7	9
Transmissive Light Efficiency (%)	Bright State	7.18	9.3	8.7	8.8	8.78	8.78
	Dark State	10	7	0.3	0.2	0.1	0
Transmissive Light Distributions (°)		29	28	31	31	31	28

3.3.2.2 IER optimization

The IER was optimized by varying the IER width (W) from 8 to 18μm while the overcoat thickness was fixed to 30 μm and EIER width to 3 μm. The results, shown in Tab. 3.3, demonstrate that the light distribution is not determined by the IER width, since the peak light intensity at various IER widths is mainly distributed at about ±30°. This distributing angle is satisfied to the requirements for the portable display applications.

Moreover, with the sequentially increasing IER width, the luminance of the transmissive mode increases gradually, as shown in Fig. 3.5. Eventually, the highest brightness of transmissive mode is achieved at IER width of 16μm. Furthermore, the contrast of transmissive mode does not vary accordingly as IER width is increased and thus the common dark state is obtained, as shown in Fig. 3.5. Thus, the optimized IER width of 16μm has been obtained for achieving high brightness and high CR of transmissive mode in the transflective Ch-LCD.

Tab. 3.3 Transmissive light efficiency and light distribution with various IER width

IER Width (μ m)		8	10	12	14	16	18
Transmissive Light Efficiency (%)	Bright State	3.26	5.33	6.73	6.25	8.72	6.79
	Dark State	0.45	0.36	0.35	0.38	0.35	0.46
Transmissive Light Distributions (°)		20	28	29	30	31	28

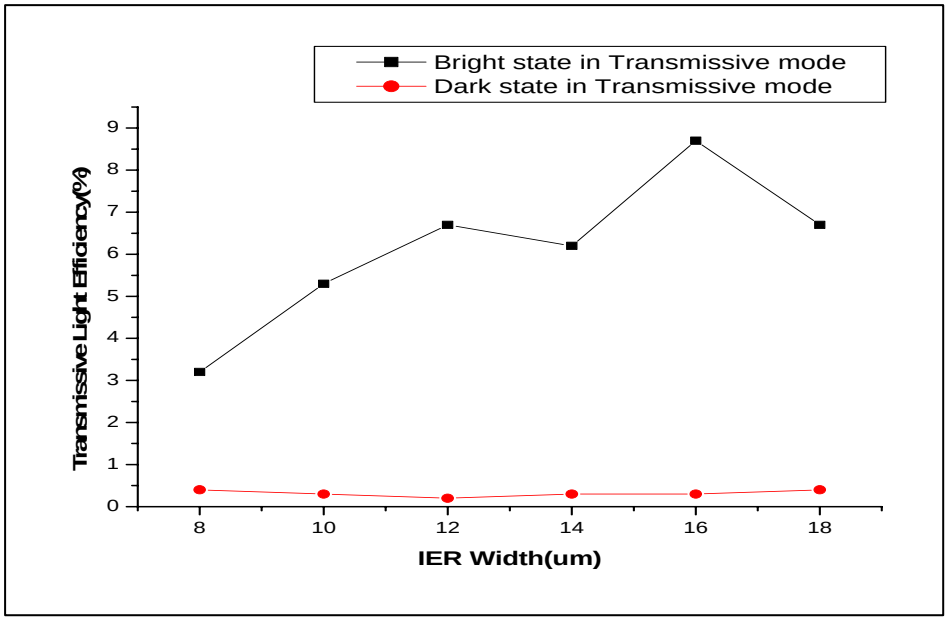

Fig. 3.5 Transmissive light efficiency in bright and dark states with various IER widths

For reflective Ch-LCD's applications, the necessary transmissive light utilization efficiency is about 30%. However, from the simulated results, the transmissive efficiency in bright state of our transflective Ch-LCD is only 8% to 9%. On the other hand, although the highest light utilization efficiency is not high enough, the transmissive efficiency of 0.3% in the dark state was achieved by the EIER structure and crossed circular polarizers. Thus, in order to have high light utilization efficiency in transmissive regions, the approach to further enhance the luminance and contrast of transmissive mode will be discussed in the following sections.

3.3.2.3 Overcoat optimization

The overcoat thickness was optimized by varying the overcoat thickness from 0 um to 1mm, whereas the IER width was fixed to 16 μm and the EIER width of 3 μm, The results, shown in Tab. 3.4, demonstrate that the light distribution is effected by the overcoat thickness. The peak light intensity is shifted from ±35° to near 0° when the thickness is increased from 0 μm to 1000 μm. This result reveals that the

collimated backlight is utilized more efficiently than that large oblique incident light, resulting in the light distribution with small viewing angle. Further, as the overcoat thickness is reduced to the distance shorter than 10μm, large oblique light is utilized more efficiently than the collimated light, resulting in the light distribution with large viewing angle.

Moreover, as shown in Fig. 3.6, the transmissive light efficiency in bright state does not increase linearly. The luminance rises as the overcoat distance between the IER and cholesteric-like reflectors increased continuously. Eventually, the peak luminance of 14 % is reached when the distance is increased to 150 μm. After that, the luminance is dropped to only 2 % as the overcoat thickness is increased to 1000 μm. According to the reflection theory, as the distance between the IER and lower reflector increased, the backlight which can be reflected to the reflective sub-pixels increases accordingly. However, if the spacing becomes too large, parts of the divergent backlight is not reflected by the IER structure, but directly transmitted through the LC layer instead.

Tab. 3.4 Transmissive light efficiency and light distribution with various OC thickness

Overcoat thickness (μ m)		0	1.5	3.5	4	6	8
Transmissive Light Efficiency (%)	Bright State	2.60	2.96	3.07	3.05	3.60	4.25
	Dark State	0.5	0.45	0.35	0.39	0.46	0.49
Transmissive Light Distributions (°)		37	31	28	28	28	25

Overcoat thickness (μ m)		10	20	40	60	80	90
Transmissive Light Efficiency (%)	Bright State	4.74	6.11	10.89	12.33	12.96	13.18
	Dark State	0.23	0.38	0.37	0.38	0.26	0.20
Transmissive Light Distributions (°)		25	29	22	21	20	19

Overcoat thickness (μ m)		100	150	200	300	400	500
Transmissive Light Efficiency (%)	Bright State	13.35	13.97	12.45	8.42	5.59	4.62
	Dark State	0.02	0.02	0.01	0.01	0.01	0.01
Transmissive Light Distributions (°)		18.35	18	15	9.03	7.04	6.56

Overcoat thickness (μ m)		550	800	1000
Transmissive Light Efficiency (%)	Bright State	4.16	2.61	1.92
	Dark State	0.001	0.002	0.001
Transmissive Light Distributions (°)		6.01	5.50	2.9

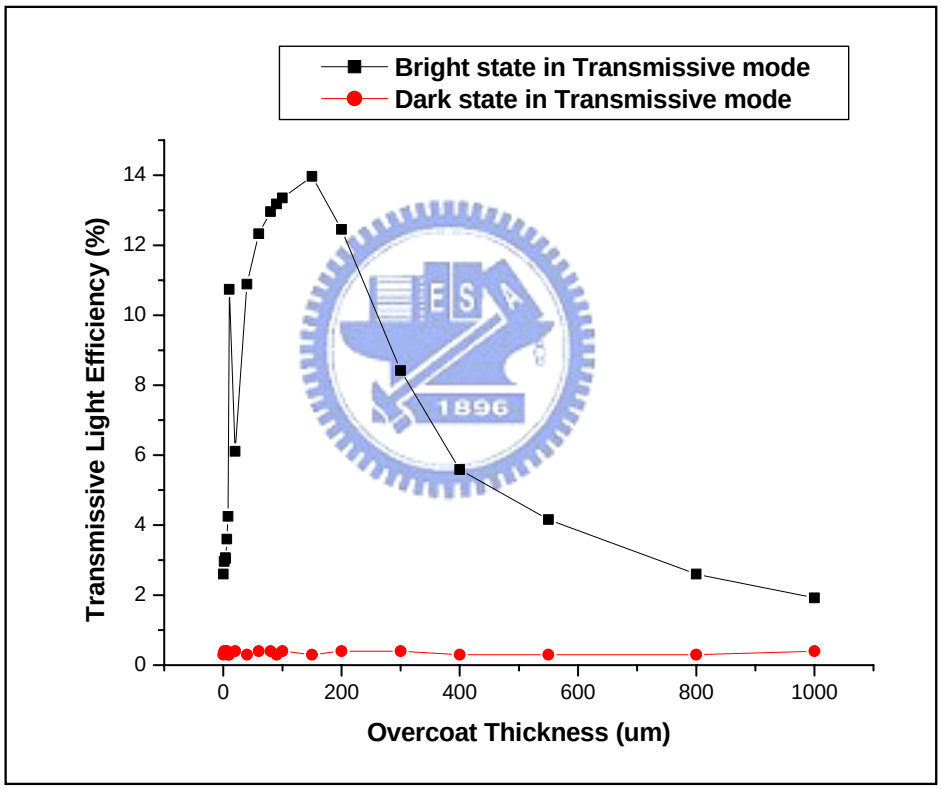

Fig. 3.6 Transmissive light efficiency in bright and dark states with various overcoat thicknesses

According to the results, the optimized overcoated thickness of 150 μm is obtained. Thus, the luminance can be enhanced by increasing the overcoat layer to over hundred micrometers. This result indicates an important application of the IER and EIER structure. Since it is difficult to spun-coat dielectric layer to such a high

thickness like 150 μm in a standard LCD process, the glass substrate of such high thickness can be used as an overcoat layer to increase the distance between the IER/EIER structures and cholesteric liquid crystal layer. Thus, the upper substrate process included IER/EIER fabrication can be viewed as a “film” structure. This film is simply laminated on the upper glass of the standard Ch-LCD without any fabrication process issue, such as glass alignment and insufficient overcoat thickness, for transflective modes application.

Finally, the result also reveals the high contrast of transmissive mode of the device is obtained, regardless of the large overcoat thickness, demonstrating that with the function of two opposite polarity circular polarizers, light leakage in the dark state of transmissive mode is diminished. Thus, without using any absorption layer required the semiconductor process, the common dark state in transmissive mode is obtained by simply using two circular polarizers with opposite polarity.

3.4 Discussions of simulation results

The result shows that the maximum transmissive luminance of 14 % is obtained, which is less than 30 % of commercial reflective Ch-LCDs. This is because the two cicular polarizers are applied in the device, thus the brightness is reduced by around 28% caused by the second polarizer (around 200 μm thick) laminating on the back substrate of the device. Moreover, the transflective Ch-LCD with side IER structure is suffered from the shadow effect shown in Fig. 3.7, and resulted in lower reflective light utilization efficiency, as compared with commercial Ch-LCD structures. However, the transmissive contrast of the proposed device is higher than the conventional reflective Ch-LCD required zero-polarizer, since two polarizers were applied to achieve common dark state, providing a perspective advantage in the future application such as RGB colors in transflective Ch-LCD.

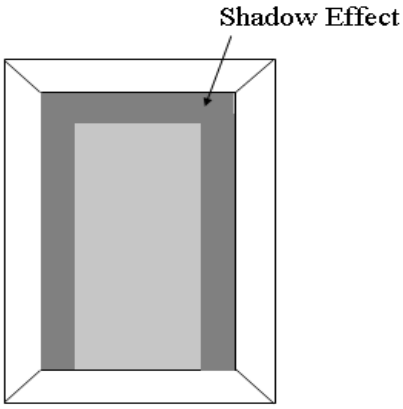

Fig. 3.7 The shadow effect of side IER structure

3.4 Summary

We successfully designed and optimized the IER/EIER structures including IER/EIER widths and distance between the IER/EIER and cholesteric layer for high transmissive light efficiency. The light utilization of side-IER configuration is not as high as we expected due to the shadow effect. The transmittance of the transmissive mode of the proposed transflective Ch-LCD is 13 %, which is lower than the reflectance of 30 % for conventional reflective ones. However, the transmissive light efficiency can be traded-off by increasing the IER width for reflective light utilization efficiency.

Furthermore, the transflective Ch-LCD is demonstrated with IER/EIER and opposite polarity circular polarizers. The luminance is primarily determined by the IER width and the overcoat thickness, whereas the contrast is mainly affected by the EIER structure and circular polarizers. Besides, the simulated results also demonstrate that the luminance and contrast of the transmissive mode is enhanced by EIER structure. Eventually, the optimized R:T ratio of 4:1 for the proposed transflective Ch-LCD is obtained by selecting IER and EIER width of 16μm and 3μm, respectively, in a pixel size of 210 x 210 μm. The simulated overcoat results also demonstrated an essential application of the IER/EIER structures. The glass can be regarded as an

overcoated layer, and thus the fabricated IER/EIER structure by the upper substrate process can be simply laminated on the conventional Ch-LCD. Besides, a high contrast in overcoat thickness over 100 μm is obtained by the optical function of these two circular polarizers with opposite polarity completely, preventing the transflective Ch-LCD from the light leakage issue. Thus, a monochromatic and full-color Transflective Ch-LCD can be fabricated with an uncomplicated process by laminating IER/EIER film and two opposite polarity circular polarizers on the conventional Ch-LCD devices.

Chapter 4

Fabrication and Measurement Instruments

4.1 Introduction

A preliminary structure will be used to confirm the features of the new transflective Ch-LCD with Image-Enhanced Reflector (IER) and Extended IER (EIER). All the fabrication technologies and instruments which are available to develop such a preliminary structure will be introduced in this chapter. The fabrication sequences of the proposed transflective Ch-LCD included the process of the upper substrate, the bottom substrate and the cell. The upper substrate process is fabricated by constructing the IER structures with the standard semiconductor process including spin coating, lithography and development. Then the reflow treatment and hard-baked process will be used to form the desired shape of the IER structure. Second, the sputtering process will be used to deposit the aluminum layer, which is used to reflect backlight of the transmission channel to the reflective region. Meanwhile, the EIER structure will be formed by this patterning process. Moreover, the transparent dielectric layer will be spun coating to form the protection layer for IER and EIER structure. Finally, ITO was deposited. For the rear substrate process, ITO and alignment layer were deposited.

The cell process joins the front and the bottom substrates with accurate alignment. The space between the two substrates was filled with cholesteric liquid crystal and spacers of 4.25 μm. Finally, two opposite handedness circular polarizers were laminated on the upper and bottom glasses. As a result, the light utilization efficiency and light distribution including a backlight and an ambient light of the transflective Ch-LCD with IER/EIER structures will be measured by the optical measurement setup.

Besides, the characteristics and performance of the fabricated optical IER structure, such as similarity to the geometric design, uniformity of surface variation were measured by typical semiconductor measurement systems like scanning electron

microscope (SEM). The major features of the above mentioned instruments will be illustrated in this chapter.

4.2 Fabrication Process

The features of the novel transflective cholesteric LCD (Ch-LCD) have been demonstrated by the simulation presented in Chapter 3. Therefore, we start to fabricate a transflective-LCD prototype to characterize the features of the proposed transflective Ch-LCD with IER/EIER structure. The whole LCD panel was fabricated to verify the optical performance according to the simulated results. We implemented our fabrication at CPT.

The detail steps to produce the prototype are listed below and the fabrication process is shown schematically in Fig. 3.1.

(a) Upper substrate process:

(1) Glass preparation: For the display application, the glass is widely used to as a substrate. In the fabrication, the sodalime double-side published glass with 0.55mm thick was chosen.

(2) Lithography process: The IER structure with desired width according to the simulated results was fabricated by standard photolithographic process. After the initial cleaning, photoresist PC403 (about 2.5μm) was coated on the glass. The photoresist PC403 was chosen to be coated on the glass substrate because this material is easy to control the pattern profile with good uniformity. Further, the photo mask was utilized to define the desired width of IER structure.

(3) Reflow and hard bake process: Three substrates were prepared on the hotplate at the reflow temperature of 135 ℃, 145 ℃ and 155 ℃ for 5 minutes in order to obtain the optimized IER structure. The sidewall

slope of the IER structure is controlled by the reflow temperature and pattern profiles will not be changed after following hard bake. Hence, reflow and hard-bake were used to make the inclined angle 15° and the residual solvent driven-off, respectively.

(4) Aluminum sputtering: After hard baking the fabricated IER structure, aluminum film was sputtered by PVD process. In order to use this bump structure in a transflective Ch-LCD, Al film is then deposited on the IER surface and patterned (2^{nd} Mask) to fabricate the extended IER (EIER).

(5) Dielectric layer coating: After forming EIER structure, a transparent dielectric layer used to enlarge the distance to the LC layer was spun coating.

(6) ITO coating: ITO film is deposited by conventional sputtering and the upper substrate process is competed.

(b) Bottom substrate process: The bottom substrate process only requires the ITO film to be deposited by a conventional sputtering.

(c) Cell process: The cell process joins the front and the rear substrate with accurate alignment. The spacer of 4.25 μm is required for achieving full color capability. Further, the space between two substrates is filled with colesteric liquid crystal. Finally, two circular polarizers with opposite handedness are laminated on the upper and rear substrates. If the cholesteric is left-handed, the left circular polarizer was laminated on the front substrate and the right circular polarizer on the bottom substrate.

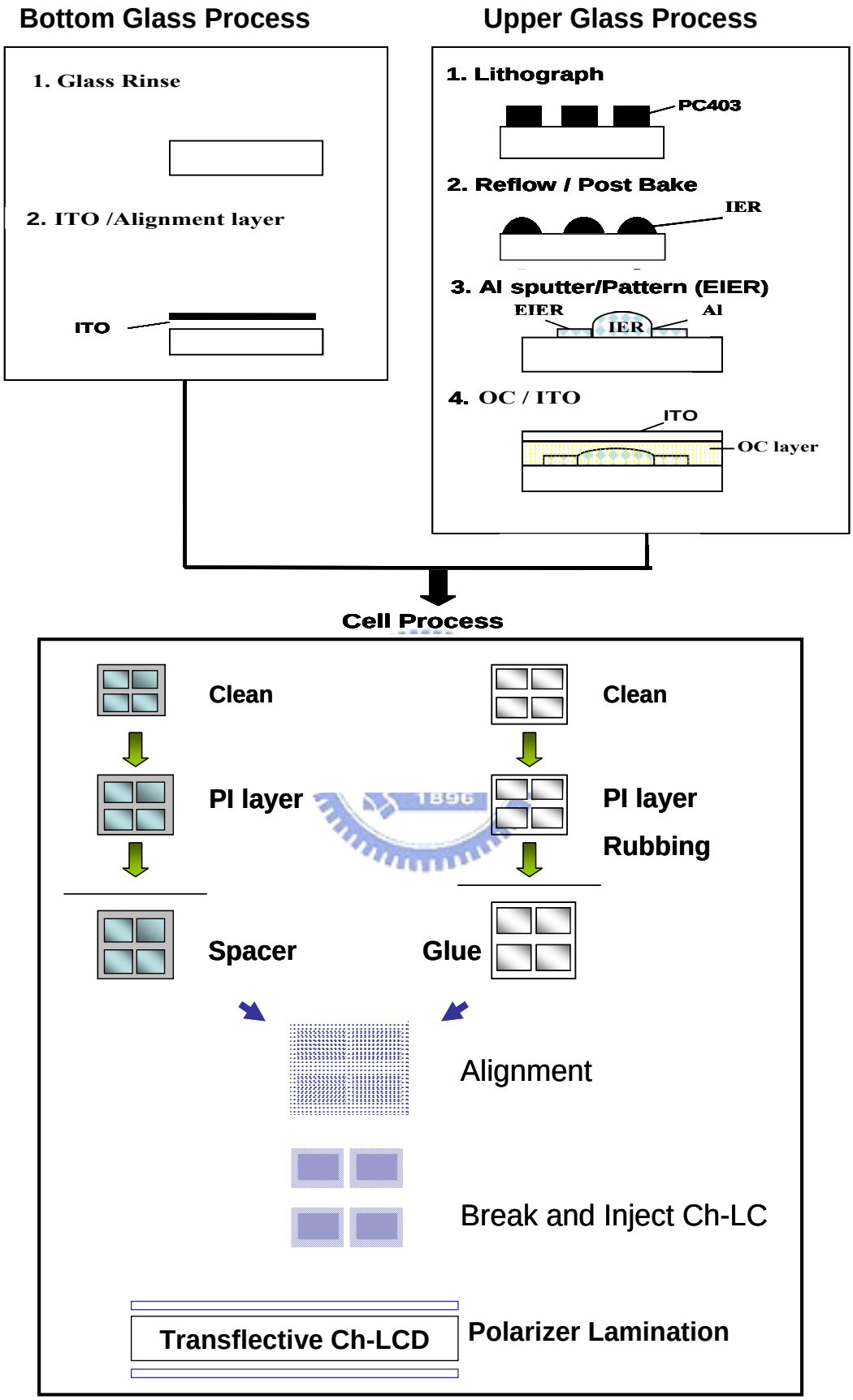

Fig. 4.1 Flow of the fabrication process for the proposed transflective Ch-LCD

4.3 Measurement System

After the fabrication of the novel transflective Ch-LCD with IER/EIER was fabricated, the inspection will be performed to make sure that the fabricated elements agree with the original design. Here, SEM will be introduced. Besides, after the fabrication process, the measurement system is necessary. Therefore, two different types of measurement systems, the Eldim EZContrast 160R (diffuse type) and LCD 7000 (collimated type) will be demonstrated.

4.3.1 Scanning Electron Microscope (SEM)

Scanning electron microscope (SEM) is an essential instrument to measure the accuracy and fidelity of the fabricated nanostructures. Using a series of electromagnetic lenses to focus the accelerated electron beam, the diameter of electron beam can be converged to the dimension of $10^{-3}\mu m$. The secondary electrons are generated where the focused accelerated electrons bombard the sample. Detecting the secondary electrons can determine the location of bombardment. Simultaneously, the focusing electron beam scans the surface of sample, with the aid of scanning coil, to map the feature of measured area, as shown in Fig. 4.2. Using SEM, the feature variation of a few angstroms can be observed. In our work, a HITACHI S-4000 SEM was used to measure the quality of our fabricated microstructure elements. The IER/EIER structures and over coated layer can be accurately measured.

Fig. 4.2 Schematic diagram of SEM

4.3.2 Optical performance measurement systems

After the preliminary fabrication of the transflective Ch-LCD with IER/EIER structures, we used two different measurement instruments to measure the luminance, contrast, colormetry, reflectance, and spectrum.

4.3.2.1 ConoScope

(a) Introduction:

The ConoScope can be used for visual performance evaluation, such as luminance, contrast ratio, color shift, gray scale and many characteristics. The basic working principle of the ConoScope is described as follows. A typical scanning device (so called "gonioscopic system") would scan the half cone above the display to detect the variations of luminance and color for each specific direction, as it can be seen in the upper right part of Fig. 4.3. Plotting each azimuthal angle on a circle was the radius from the center additionally indicates the polar angle results in the so called polar coordinate system. This is shown in the left upper part of Fig. 4.3. Using such a

polar plot to mark for each direction luminance and / or color will result (in the case of color) a colored figure as it is shown in the lower part of Fig. 4.3

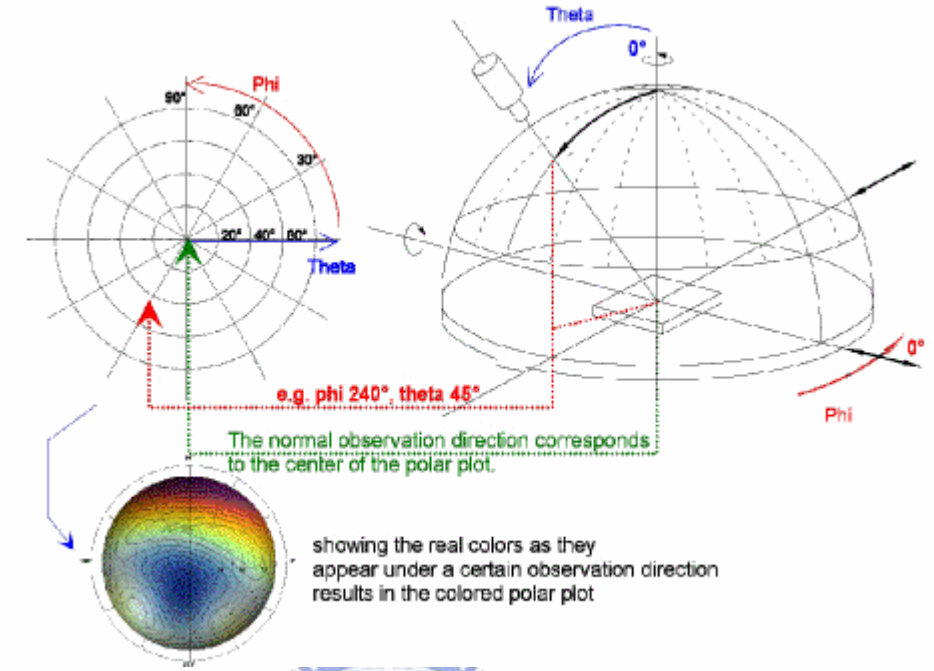

Fig. 4.3 The concept of a conoscopic receiver.

An arrangement of several lenses (here represented by one single lens) modifies the light propagation directions in a way, that all beams emerging from the sample in the same direction will meet in one spot in the so called focal plane. The ConoScope lens projects all parallel beams on one spot in the focal plane. The resulting figure is called the "conoscopic figure". This means, that each spot on the focal plane (or within the "conoscopic figure") corresponds to one specific direction of the viewing cone. The conoscopic figure directly shows color and luminance as they would have been plotted in a polar coordinate system as described under figure 4.4. In our measurement, we used the collimated illumination as the backlight for the transmissive modes and ambient light for the reflective mode to analyze the luminance, contrast ratio, spectrum and light distribution of the transflective Ch-LCD.

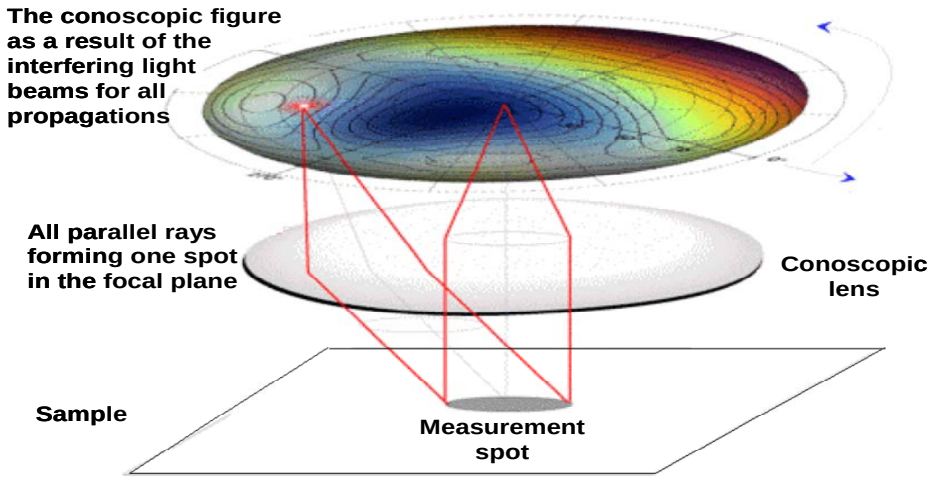

Fig. 4.4 Illustrations of ConoScope detector.

Chapter 5

Experimental Results

5.1 Introduction

The features of the novel transflective cholesteric LCD (Ch-LCD) have been demonstrated by the simulation. Therefore, we start to fabricate a transflective-LCD prototype to characterize the features of the new transflective Ch-LCD with IER / EIER structures in two different processes (Inner IER and Outer IER processes). The whole LCD panel was fabricated to verify the optical performance according to the simulated results presented in Chapter 4.

5.2 IER/ EIER Fabrication Results

In this section, two fabricated results from the inner IER and the outer IER process will be demonstrated. For the inner IER process, as shown in Fig. 5.1(a), the IER was initially designed to fabricate inside the device, therefore, the overcoat layer and ITO were required for forming spacing to Ch-LC and the electrode, respectively. For the outer IER process, as shown in Fig. 5.1(b), the IER was extended to fabricate outside the device and then laminate on the upper substrate of the Ch-LCD, thus in this process overcoat layer and ITO were not required but the passivation layer using SiNx was deposited. Further, since the material (PC403) to form bump-shaped IER was not compatible to TFT process line, thus to reduce the cost and facilitate the process, a flat-shaped IER was designed and the fabrication process as well as the comparison between the bump-shaped IER and Flat-shaped IER will be performed.

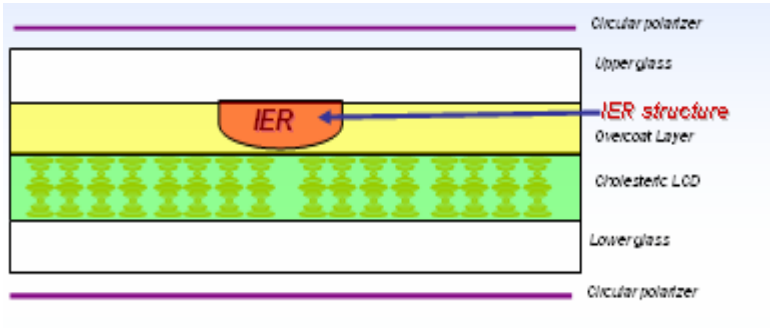

(a)

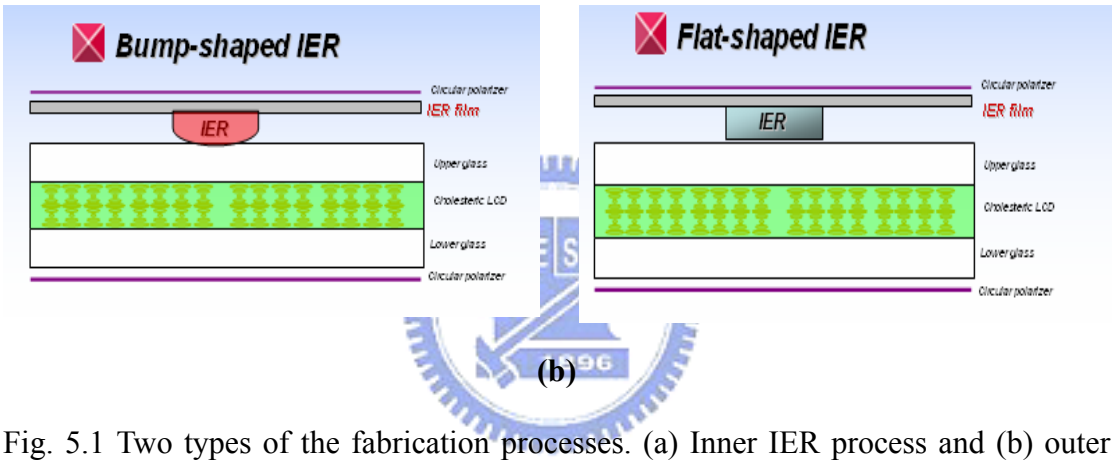

(b)

Fig. 5.1 Two types of the fabrication processes. (a) Inner IER process and (b) outer IER process.

5.2.1 Inner IER Process

The inner bump-shaped IER structure was fabricated by photolithography process with additional reflowing treatment (1st mask) on the hotplate. Then, EIER was fabricated by the sputtering process (2nd mask). Further, the overcoat layer was achieved by using PC403 to create spacing between bump IER to cholesteric by 2.5μm. Finally, ITO was sputtered at 1000Å. The parameters chosen for the IER fabrication were listed in the Tab.5.1.

Tab.5.1 Process flow and condition of IER fabrication

Process	Condition
Coating	spin coating
Softbake	90˚C / 2 min hotplate
Exposure	ghi line 2450 msec
Development	Developer: 0.4%TMAH
Rinse	Runnuning DI water:60 sec
Reflow	130 -150 ° C / 2 min hotplate
Hardbake	220˚C / 1 hr / Oven

The IER height was mainly determined by the coating photo-resist (PR) thickness and exposure time. In order to obtain the desired IER height, thus the optimized process parameters including coating thickness, its corresponding spin speed, and exposure time were needed to be determined. The desired IER height was 2.2μm and since the re-flow treatment could contribute to the reduction of IER height to roughly a few micrometers, thus the PR coating was coated to 2.5μm. Further, to obtain the desired height, the relationship between the PR thickness and spin speed was modeled. The spin time was fixed to12 sec and pre-baked temperature at 90˚C, whereas the spin speed was increased from 700rpm~1300rpm. The condition for spin speed at 12 sec is shown in Tab. 5.2.

Tab. 5.2 Parameter condition at spin time of 12 sec

Parameter	Condition
Pre-baked Temp.	90˚C / 110 sec
Spin time	20 sec
Spin speed	700/ 900 / 1100/ 1300 rpm

The result showed that the PR thickness was varied in a range from 41518 Å to 25281 Å corresponding to the spin speed from 700 to 1300 rpm, as shown in Fig. 5.2. As these data suggested, the desired IER of 2.5μm was obtained at a spin speed of 1300 rpm.

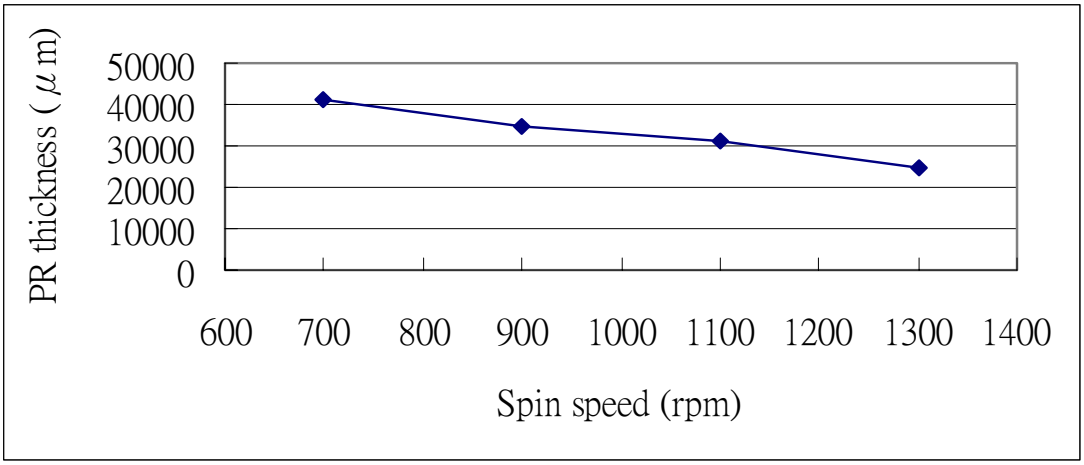

Fig. 5.2 Relationship between the PR thickness and spin speed

After the glass substrates were spun coated with photoresist PC 403 and exposure by the g line at 2450 msec as well as developed by 0.4% TMAH, the photoresist was necessary to be reflowed for forming the bump-shaped IER. Since the reflowing temperature affected the properties of the photoresist for fabricating the IER bump-shaped structure, hence we prepare three kinds of substrates for obtaining the desired IER height and width as well as tilt angle by reflowing the photoresist on the hotplate for 135° C, 145° C and 155° C at 2 minutes. Fig. 5.3 demonstrated the fabricated bump-shaped IER results after the reflowing process measured by OM. In order to use this bump structure in a transflective Ch-LCD, Al film was then deposited on the IER surface and pattered (2^{nd} mask) to fabricated the extended IER (EIER). The fabricated IER/EIER measured by OM was shown in the Fig. 5.4.

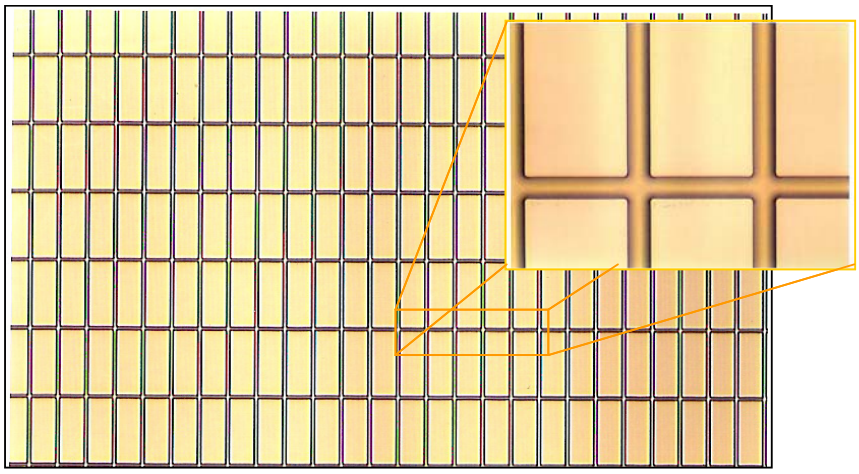

Fig.5.3 Fabricated IER measured by an OM after reflowing process

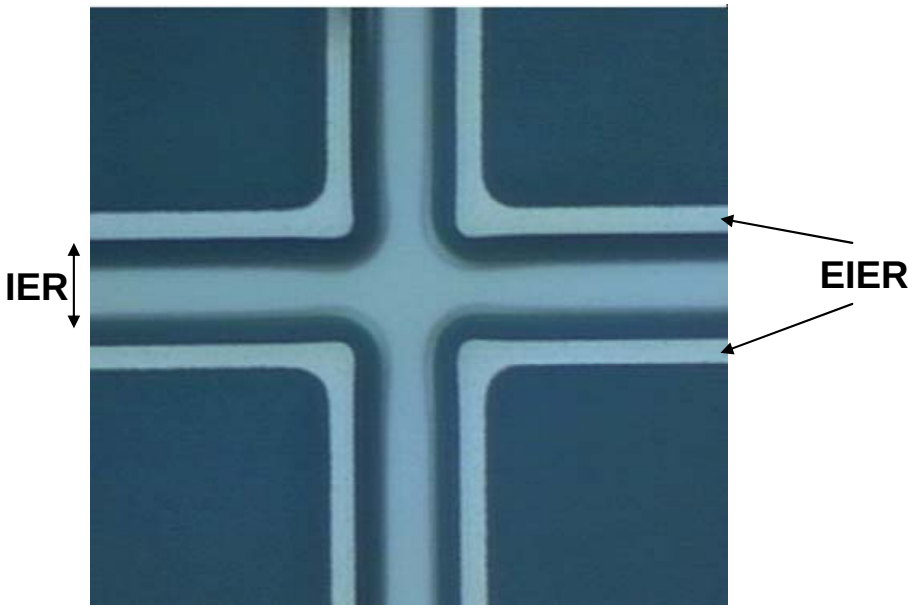

Fig.5.4 Fabricated EIER measured by an OM after the patterning process (2nd mask)

Finally, an overcoat (OC) layer was spun coated to increase the spacing between IER and cholesteric cell. The organic PC403 was selected since it can provide high transmittance up to 96% after exposed by g line at 300J/cm^2. Since this bump-shaped IER structure was initially designed in the inner cell, therefore, ITO was then deposited by conventional PVD process and the process was completed.

The fabricated inner bump-IER results at the reflowing temperature of

135°C, 145° C and 155° C measured by SEM were shown in Fig 5.5, Fig.5.6 and Fig.5.7, respectively. If the photoresist was only melt-baked at 135° C, the measured width and measured height are 16.98μm and 2.113μm, respectively. Then as the reflowing temperature was increased to 145°C, the measured IER width and height were increased to 17.09μm and 2.262μm, respectively. On the other hand, if the reflowing temperature was increased to 155°C, the IER width was continuously extended to 17.12μm, while the IER height was reduced to 2.106 um.

Tab. 5.3 Measured results of IER structure at different reflowing temperature

Temperature(°C)	IER height (μm)	IER width (μm)
135	2.113	16.98
145	2.262	17.09
155	2.196	17.12

Tab. 5.3 summarized the measured results at different reflowing temperatures. The results of this study demonstrated that IER widths in three substrates were increased from 14μm (after lithography) to 17μm by the reflow process, which was not exactly but closed to the desired value of 16 um. Further, after the reflow process the photoresist with three different kinds of baking conditions can be fabricated with good shape. This is because solvent in the photoresist had been vaporized by soft-baked process at 90 °C, which made the photoresist suitable for the fabrication. However, we found that the shape of the IER structure at melt-bake temperature of 145 ° C was sharper than those of 135 ° C and 155 ° C. Further, the Al on the top of bump-IER structures was peer-off, which seriously affected the optical performance at normal direction. Besides, the tilt angles of the three bump-IER structures at different reflowing temperatures were tilted at around 30˚, which did not

agree to our initial design of 15˚. To solve the issue, raising temperature on the hot plate was required. Nevertheless, the optimum reflowing temperature cannot exceed 155˚C, since the maximum temperature of the hot plate was only 180˚C. Therefore, extending the reflowing time at certain temperature was the only solution to obtain the desired tilt angle. Further, to simply the fabrication procedure and be more compatible to the TFT-process line, an alternative IER called flat-shaped IER was fabricated.

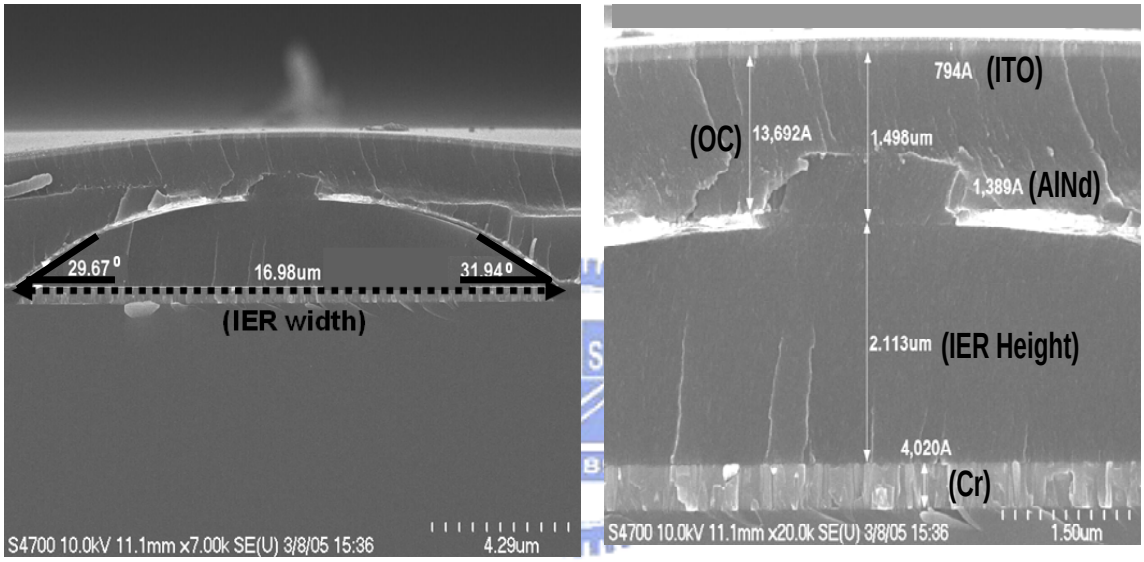

(a) **(b)**

Fig.5.5 Inner bump-IER structures measured by SEM at reflowing temperature of 135 ° C. (a) IER width and tilt angle and (b) thickness of each layer

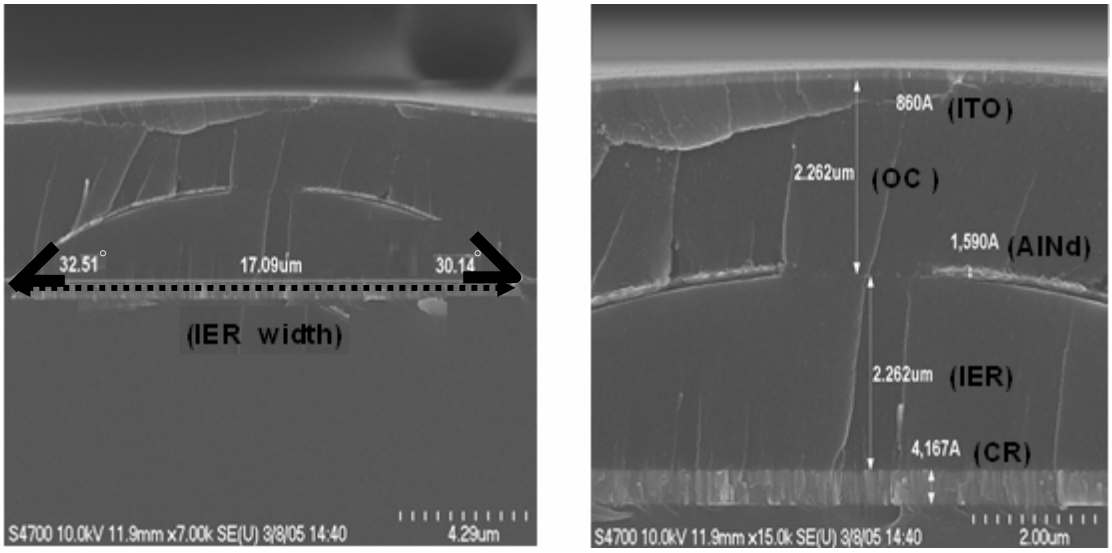

(a) **(b)**

Fig.5.6 Inner bump-IER structure measured by SEM at reflowing temperature of 145°C. (a) IER width and tilt angle and (b) thickness of each layer

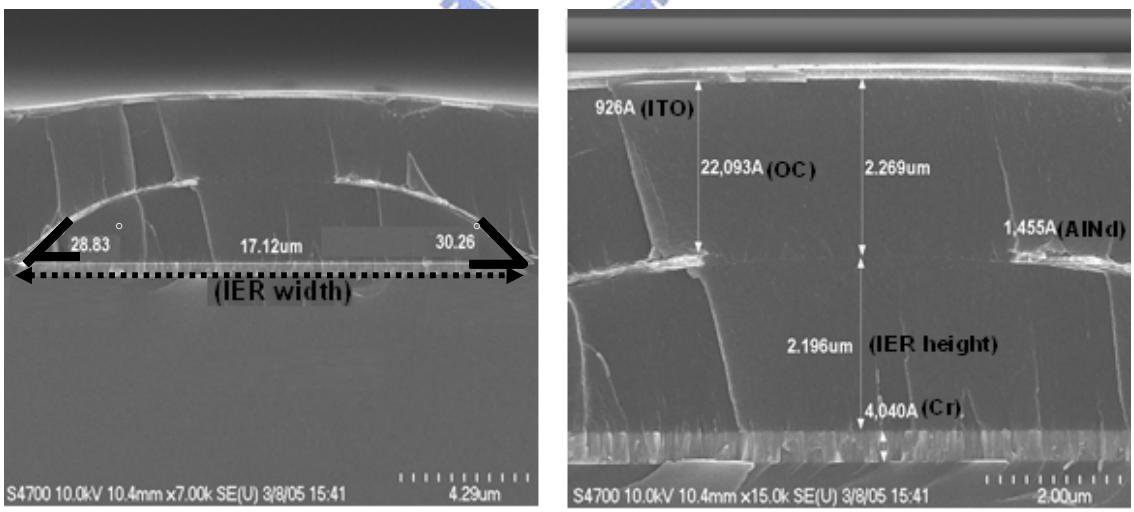

(a) **(b)**

Fig.5.7 Inner bump-IER structure measured by SEM at reflowing temperature of 155°C. (a) IER width and tilt angle and (b) thickness of each layer

5.2.2 Outer IER Process

In the previous section, the undesired IER shape was obtained and the Al was peered off on the top surface of IER structure. To solve these issues, the fabrication process was modified by extending the reflowing temperature from 2 minutes to 5 minutes to obtain the desired profile of bump-IER. Further, to simply the fabrication procedure and be more compatible to the TFT-process line, an alternative IER called flat-shaped IER was fabricated.

5.2.2.1 Outer Bumped-shaped IER

The outer bump-shaped IER structure with improved process was fabricated the same procedure as in the inner-IER experiment except the reflowing temperature was extending from 2 minutes to 5 minutes. The outer bump IER first fabricated by photolithography process with additional reflowing treatment (1^{st} mask) on the hotplate. Unlike the first experiment, the reflowing temperature at 140˚C was increased from 2 min to 5 min. Then, EIER was fabricated by the sputtering process (2^{nd} mask). Further, unlike the inner IER experiment, the overcoat process was achieved by deposing SiNx as passivation layer to 3000Å. SiNx was selected since it was highly compatible to the fabrication line as well as preserving the characteristics of high transmittance. The parameters chosen for the IER fabrication were listed in the Tab.5.4.

Tab.5.4 Process flow and condition of outer IER fabrication

Process	Condition
Coating	spin coating
Softbake	90˚C / 2 min hotplate
Exposure	ghi line 2450 msec
Development	Developer: 0.4%TMAH
Rinse	Runnuning DI water:60 sec
Reflow	140 ° C / 5 min hotplate
Hardbake	220˚C / 1 hr / Oven

The fabricated result of outer bump-IER was demonstrated in the Fig. 5.8. The results of this study showed that IER widths of 15.36μm and right-side tilt angle of 15.38º were obtained. Therefore, the tilt angle was reduced from 30º to 15º when the reflowing temperature was extended from 2 minutes to 5 minutes. Nevertheless, on the right side of the IER, the tilt angle of 18.77º did not agree with the desired value. Thus, the results revealed that the reflowing rate was unequal on the both side of IER. Further, the desired IER height was 2.2μm, yet the fabricated IER width was 2.83μm. After all, the Al was not split after PVD process. The Al was not split because the IER structure was immediately sputtered by the Al, and hence remaining good adhesion between these two materials. In summary, the outer bump-IER generally agreed with the design structure.

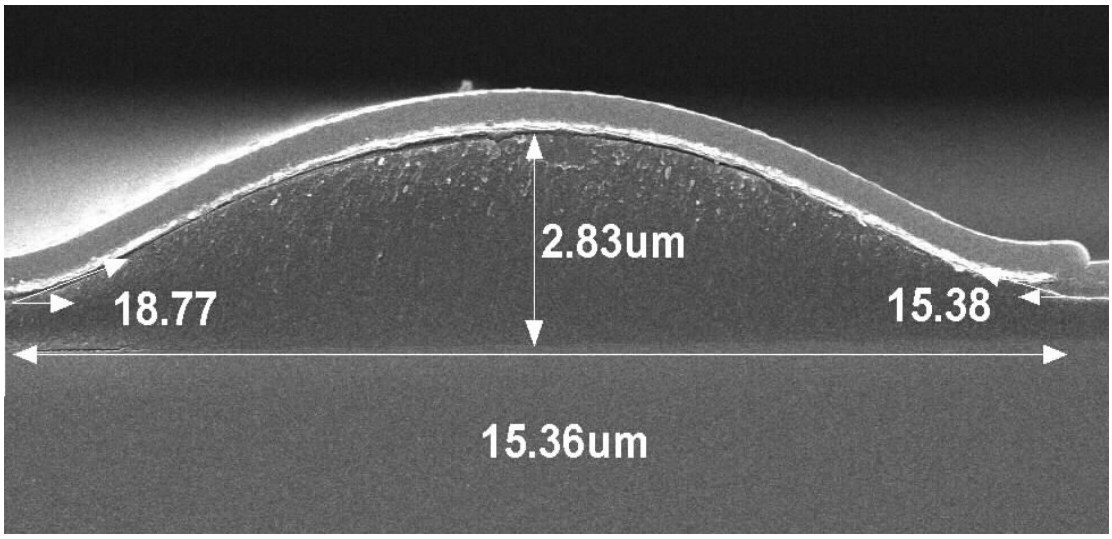

Fig.5.8 Fabricated results of the bump-IER structure with improved process measured by SEM at reflowing temperature of 140° C

5.2.2.2 Flat-shaped IER

The purpose of this experiment was used to compare the optical performance and fabrication process of Flat-IER with the bump IER. The flat-shaped IER was fabricated by the conventional sputtering the process (2^{nd} mask). The fabricated results of the flat-shaped IER were shown in Fig. 5.9. We fabricated the sample with the total width (width of IER plus width of EIER) of 27.16μm, where the designed width (width the bump-shaped IER of 16μm plus two EIER widths of 10μm) was 26μm. It was obvious that the flat-shaped IER was fabricated with the simpler process as well as more suitable to the TFT-LCD fabrication line when compared with the bump-shaped IER, since the flat-shaped IER only required conventional PVD process to deposit the Al film and then use pattering process with one mask to define its width. The optical performance of flat-shaped IER as well as bump-shaped IER in different OC thickness will be compared and demonstrated in the following sections.

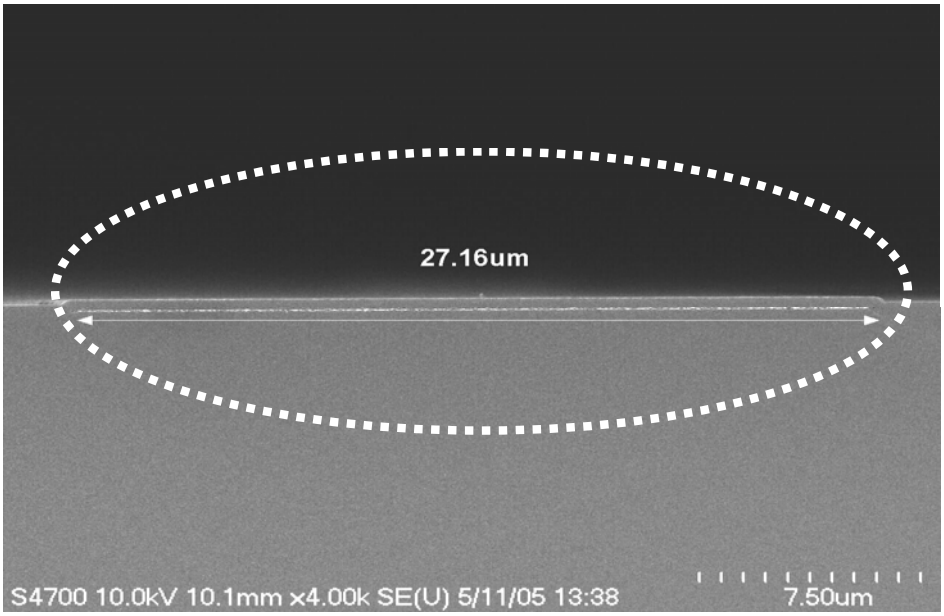

Fig.5.9 Fabricated results of the flat-shaped IER structure with improved process measured by SEM.

5.3 Optical Evaluation of transflective Ch-LCD with IER

The cholesteric liquid crystal provided by Merck (FM-M01) with the center wavelength at 550 nm (narrow bandwidth) was provided to inject into the cell, thus only the green light will be reflected. Various optical measurements of the transflective Ch-LCD fabricated with internal IER structure (OC = 2.5 μm) as well external IER structure (OC = 600 μ) will be performed and compared. The device was measured under normal incidence, where $\theta p = 0^\circ$ and Φp = 0° . Finally, the comparison between our device with the simulated results as well as CPT's reflective Ch-LCD will be discussed.

5.3.1 Luminance and CR

Three parameters including IER width, EIER width and overcoat (OC) thickness will be used to analyze the light efficiency and CR in both transmissive and reflective modes of the transflective Ch-LCD. As a result, the relationship among

them will be demonstrated, as compared to the simulated results.

5.3.1.1 Effect of IER on Luminance and Contrast Ratio

We first study the effect of bump-IER structures on the light efficiency and CR of our transflective Ch-LCD in both transmissive and reflective modes, the relationship between IER and light efficiency as well as CR at OC = 600μm and OC = 2.5μm in both modes were measured.

In the transmissive mode, the EIER width was first fixed to 5μm and the width of IER was varying from 10 to 20μm. Under the fixed EIER width, the transmittance at OC thickness of 2.5μm increased gradually with the sequentially increasing IER width and then decreased after passing certain IER width, which follows the similar trend as in the simulation results as shown in Fig. 5.10(a). Thus, at OC = 2.5μm, the highest transmittance of nearly 2 % was achieved at IER width of 14μm.

As the OC thickness is increased to 600μm, the transmittance did not obviously increase while raising IER width, and thus did not follow the similar trend of the simulation result. At OC = 600μm, the highest transmittance of nearly 3% was achieved at IER width of 14μm.

Furthermore, the contrast ratio at both OC thickness did not vary accordingly as IER width was increased and thus does not follow the same trend as in the simulation results. At both OC thicknesses, the highest CR of 5:1 was obtained at the IER width of 14μm, as shown in Fig. 5.10(b). The results demonstrated the highest transmittance were measured at the IER width of 14μm under two different OC values, as compared to the highest simulated transmittance at IER width of 16μm.

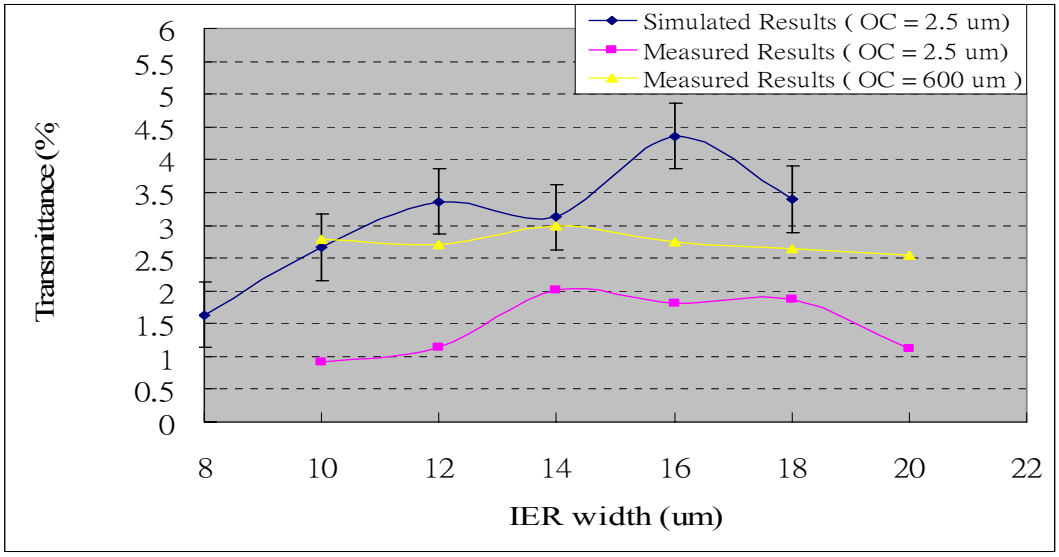

(a)

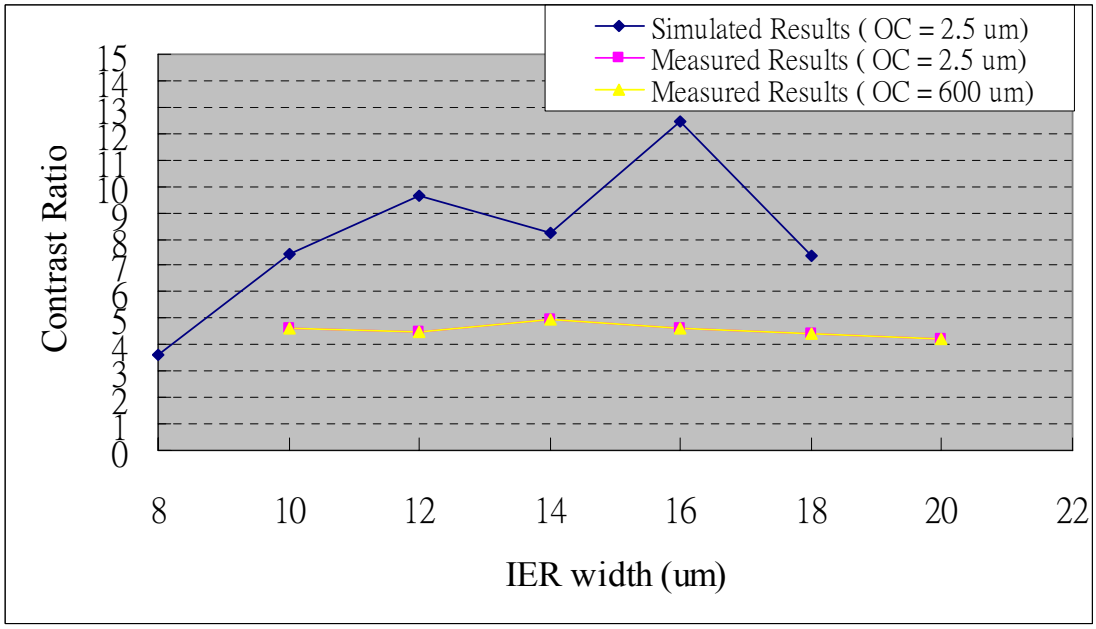

(b)

Fig. 5.10 Measured (a) transmittance and (b) CR with various inner-IER width in the transmissive mode of translfective Ch-LCD

In the reflective mode, the EIER width was first fixed to 5μm and the width of IER was varying from 10 to 20μm. Under the fixed EIER width, both the reflectance and CR were slightly influenced by the various IER widths, as shown in Fig. 5.11.

The results also indicated that maximum reflectance and CR were occurred at the IER width of 14μm. Thus, to obtain the highest luminance and CR in both reflective and transmissive modes, the IER width of 14μm was selected.

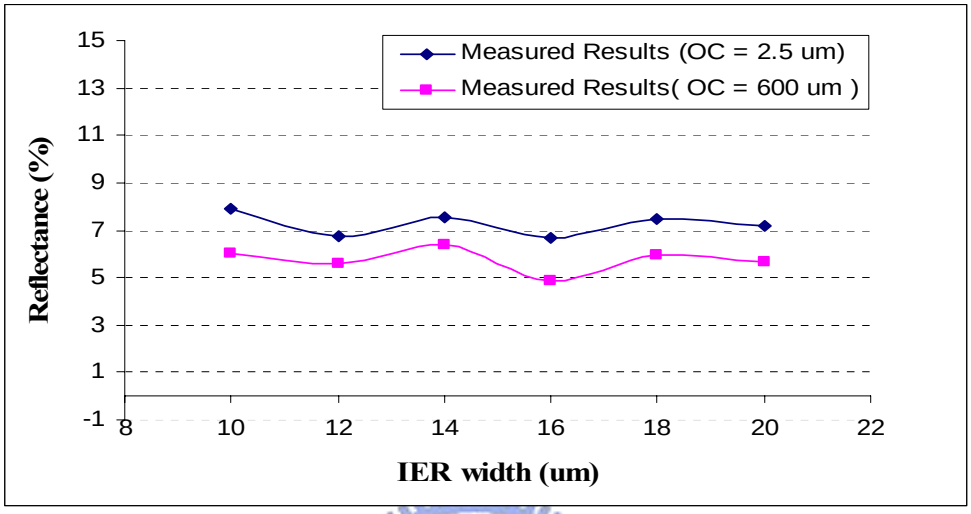

(a)

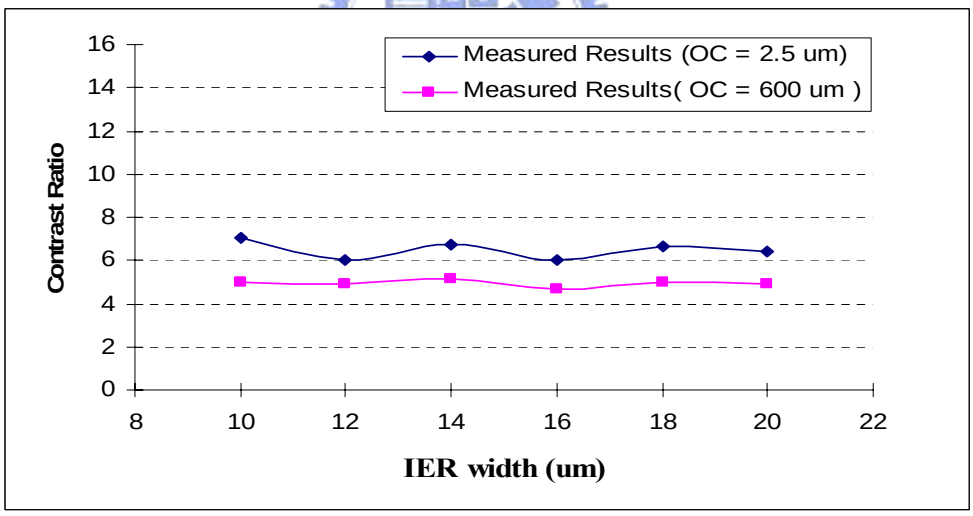

(b)

Fig. 5.11 Measured (a) reflectance and (b) CR with various IER width in the reflective mode of translfective Ch-LCD

5.3.1.2 Effect of EIER on Luminance and CR

To observe the effect of EIER structures on the light efficiency and CR of our transflective Ch-LCD in both transmissive and reflective modes, the light efficiency

and CR at OC = 600μm in both modes were measured, and the results were summarized in Tab.5.5

Tab. 5.5 Measured Efficiency and CR in reflective and transmissive with various EIER width

Sample : IER = 16 um	**OC = 600 um**	
EIER width (um)	3	5
Reflective efficiency (%)	9	6
CR in reflective mode	6:1	5.4:1
Transmissive efficiency (%)	2.5	2.8
CR in transmissive mode	4.1:1	4.7:1
Total efficiency (%)	11.3	8.8

The IER width was first fixed to 14μm and the effect of EIER was observed by varying its width from 3μm to 5μm. In the transmissive mode, both results measured under different OC thickness demonstrating that the transmittance and CR were enhanced while increasing the EIER width. Thus, EIER was provided to enhance the transmittance by using the oblique incident light more efficiently and increase CR by preventing the dark state from occurrence of light leakage. As a result, the measured results agreed with the simulated results shown in Fig.3.4. Further, in the reflective mode, with the sequentially increasing EIER width, the reflectance and CR decreased gradually. This is due to the reflective area was reduced when EIER was increase, and thus the reflectance was compensated by increasing the transmittance. As a result, with the sequentially increasing EIER width, the transmissive efficiency increased slowly while the reflective light efficiency decreased gradually. To obtain high

luminance and CR for outer IER usage, the EIER of 3μm should be selected since the total efficiency was higher than that of 5μm.

5.3.1.3 Effect of Overcoat thickness on luminance and CR

To observe the effect of overcoat (OC) thickness on the light efficiency and CR of our transflective Ch-LCD in both transmissive and reflective modes, the light efficiency and CR at OC = 600μm in both modes were measured. The IER and EIER width was first fixed to 16μm and 3μm, respectively, and the effect of OC on light efficiency and CR was measured by varying its thickness from 2.5μm, 150μm to 600μm. Recall that OC = 150μm performed the optimized transmittance in the simulation results. In the transmissive mode, Fig.5.12 demonstrated the transmittance and CR were varied accordingly to the OC thickness. The highest transmittance as well as CR was obtained at OC = 150μm. The measured results essentially followed the similar trend as in the simulated results. However, the transmittance of 3.4% at OC = 150μm did not consent to our optimized design of 14% transmittance obtained in the simulated results. This is might resulted from the unmatched index between each layer as we constructed the IER outside panel, thus the light will encountered various of refraction when propagating into different media with unmatched index. Therefore, the index matched glue should be applied in order to solve the issue. Nevertheless, the measured result was principally followed the similar trend as in the simulated results.

Further, in the reflective mode, with the sequentially increasing OC thickness, the reflectance and CR decreased gradually, as shown in Fig.5.13. Thus the reflectance and CR was mainly affected by the OC thickness.

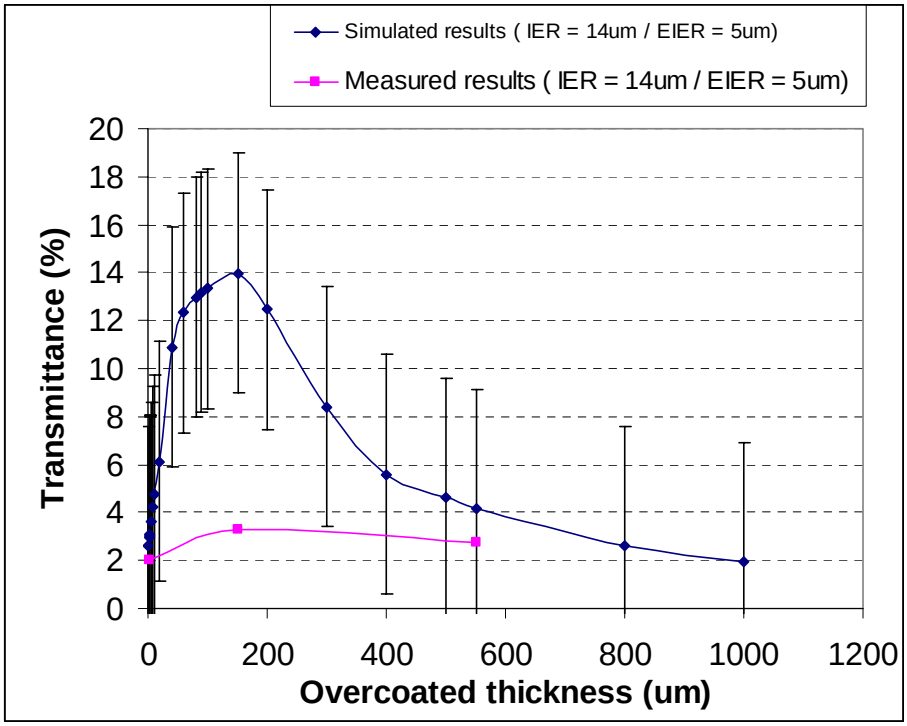

(a)

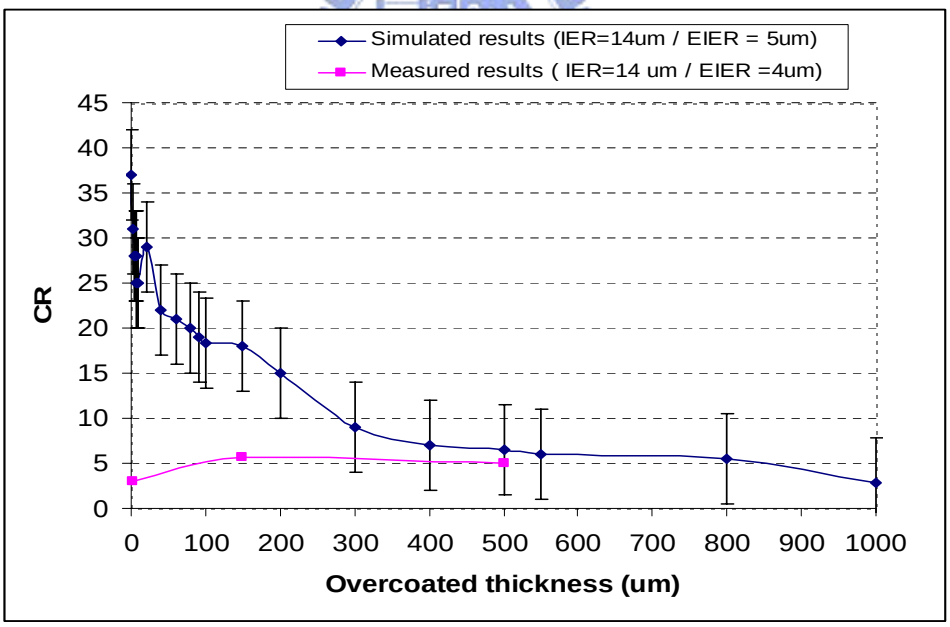

(b)

Fig.5.12 Measured (a) transmissive efficiency and (b) CR with various OC thickness (under inner IER process)

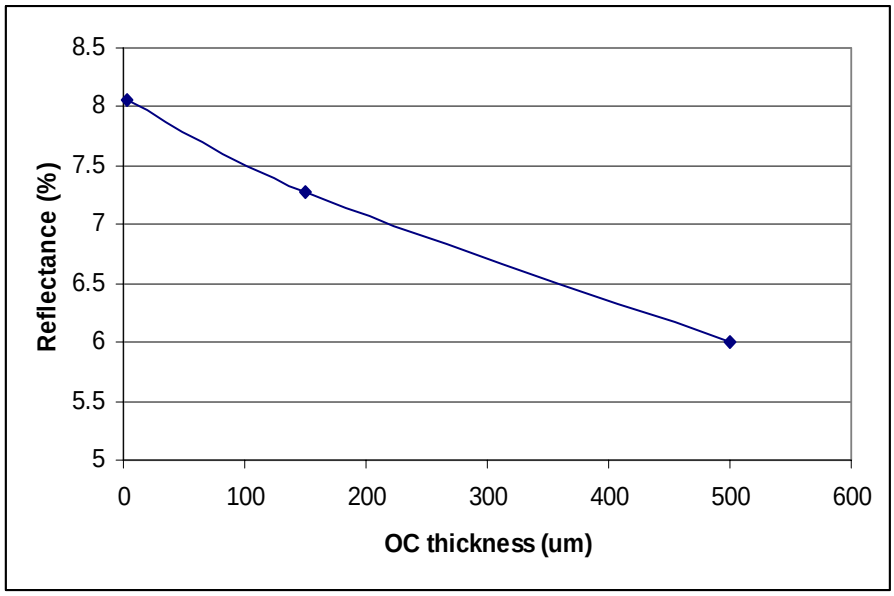

(a)

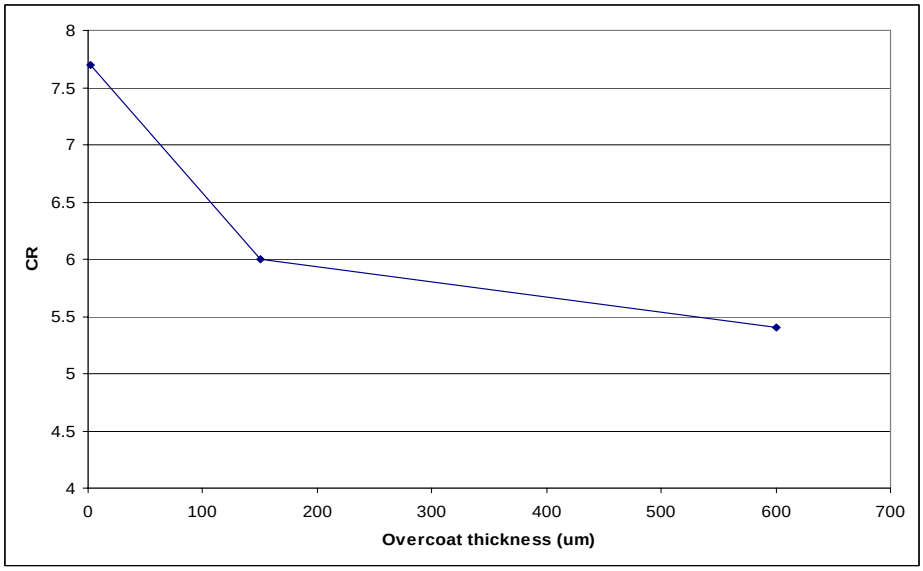

(b)

Fig.5.13 Measured (a) reflective efficiency and (b) CR with various OC thickness (under inner IER process)

5.3.2 Light Distribution

In this section, we will use IER, EIER and OC thickness to study the light distribution of the transflective Ch-LCD in both reflective and transmissive modes.

5.3.2.1 IER versus Viewing Angle and Light Distribution

To observe the effect of IER width on the light distribution in both transmissive and reflective modes, the OC thickness was fixed to 600μm and EIER width to 5μm. The backlight with maximum flux of 12000 nits was provided. As shown in Fig.5.14, the results demonstrated that the light distribution spreads in the similar fashion at various IER widths. At each IER width, the peak luminance of 8% was retained at the angle of nearly $\pm 60^{\circ}$, whereas at the normal direction the transmittance was maintained only at about 2.5 to 3%.

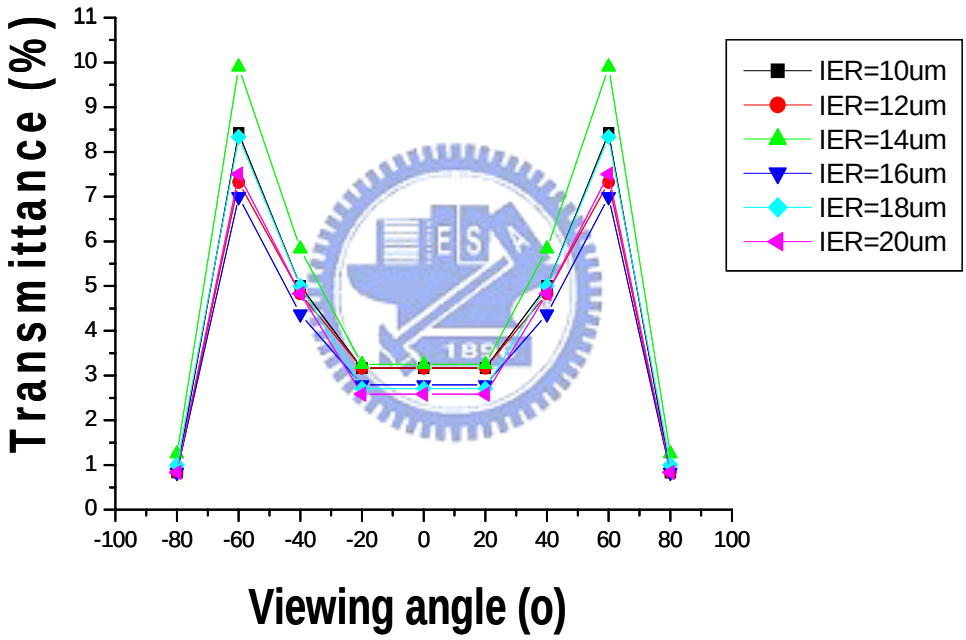

Fig.5.14 Measured light distribution at various IER width in transmissive mode

In the reflective mode, the effect of IER on the light distribution was measured by fixing the OC thickness to 600μm and EIER width to 5μm. The reference light with the luminance of 300 nits was provided. Fig.5.15 demonstrated that the light distributing was not varied while increasing the IER width. Further, the peak reflectance was mostly distributed at the normal angle, whereas the transmissive light distributed its peak values at the oblique angle, thus the device in the reflective mode

is expected to yield better image than the one in the transmissive mode.

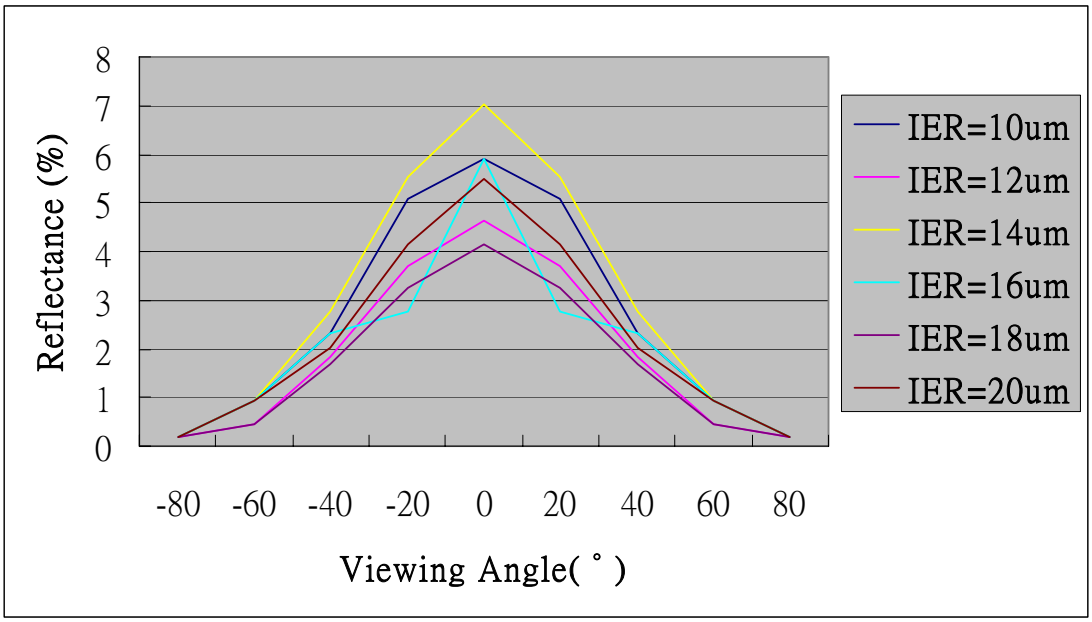

Fig.5.15 Measured light distribution at various IER width in reflective mode

As we compared the light distribution between transmissive and reflective modes, it is acknowledged that the only transmissive light was affected by the IER structure whereas the reflective light was independent from the IER. In the transmissive mode the backlight was reflected first by IER then used the Bragg reflection of Ch-LC to viewer. Thus, the transmissive light required twice reflection to the observer, whereas the reflective mode light only needed Bragg reflection to arrive at the spectator. Thus, IER did not caused major influence in the reflective mode.

To raise the transmittance at the normal angle, following factors were considered to analyze the light distribution. The IER profile, shown in the outer IER process in the previous section, demonstrated that the tilt angle of 15° was closely agreed to the desired design. According to the simulation results, the light distribution at IER tilt angle of 15° should be resulted in the viewing angle of ±30°, yet the measured results demonstrated that the peak transmitted light was spread at ±60°. Thus, we

assume that the tilt angle might not be the main factor for raising the transmittance around the normal angle (-30˚ to +30˚). To further examine this assumption, we compared the bump-shaped IER with flat-shaped IER constructed externally on the upper substrate. As shown in Fig. 5.16, the result demonstrated that even the peak transmittance of the flat-shaped IER was distributed at ±60˚. Thus, we can conclude that the tilt angle of the bump-IER was not the essential factor to influence the light distribution. Therefore, it can be predicted that the unmatched index between different layers can be considered as another factor responsible for such low light efficiency at the normal viewing angle.

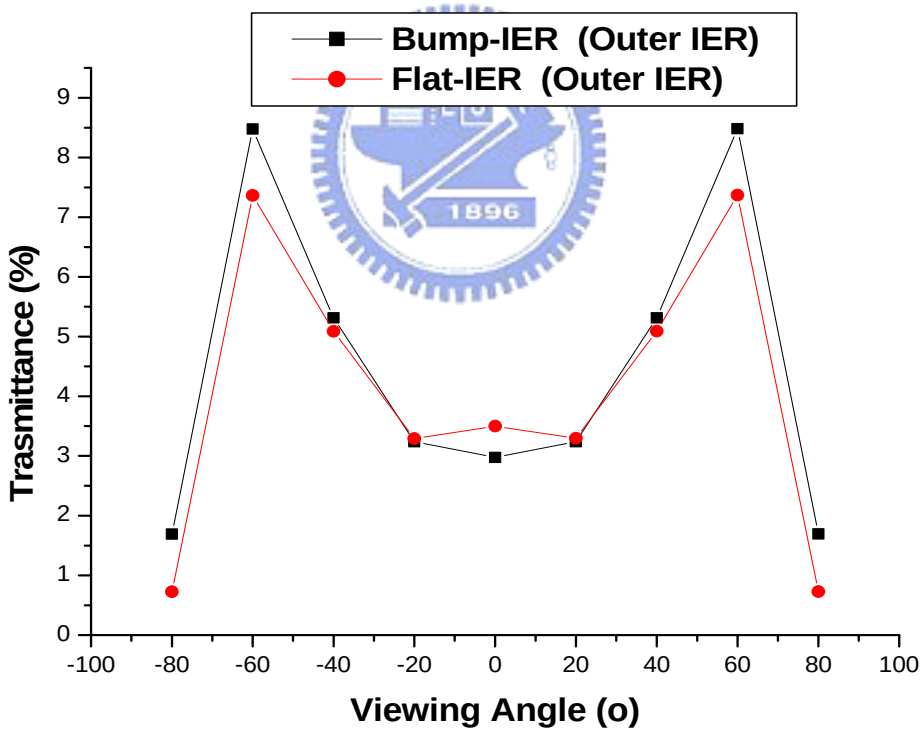

Fig.5.16 The comparison of the light distribution between flat-and bump-IER in transmissive mode

5.3.2.2 Effect of Overcoat on Viewing Angle and Light Distribution

To observe the effect of OC on the light distribution, the OC thickness was measured at 0.25μm and 600μm. The results demonstrated the transmittance of both bump–IER in the normal direction has increased from 0.5 % to 3% by raising the OC from 2.5μm to 600μm, as shown in Fig. 5.17. This is due to that transmittance at normal direction can be utilized more efficiently when the OC thickness was increased. For instance, assume cholesteric LC was left-handed material and consider OC thickness was 2.5μm, the backlight from normal angle first transformed into R light by RCP, and become the L light upon the reflection on the IER. Due to the OC thickness was insufficient, thus the 2nd reflection on IER or EIER was occurred after Bragg reflection, thus the polarity will become R light opposite to the cholesteric LC and the backlight will transmit through the LC layer, resulting in the low light efficiency at the normal angle.

Further, since the cholesteric device has the bandwidth at 550 nm, Fig. 5.18 demonstrated colorimetric evaluation, in which the color was shifted from reddish to the desired color (green) by increasing the OC thickness. Thus, the reflective and transmissive light displayed the same image color in the bright when the OC thickness is increased to OC thickness of 600μm, which is equivalent to the glass thickness. Thus, IER structure can be constructed on the upper glass, and the IER film was realized to display the color in bright state under any ambience. In the following section, we will use spectrum to demonstrate that the transmissive and reflective modes can display same bright and dark state under any ambience.

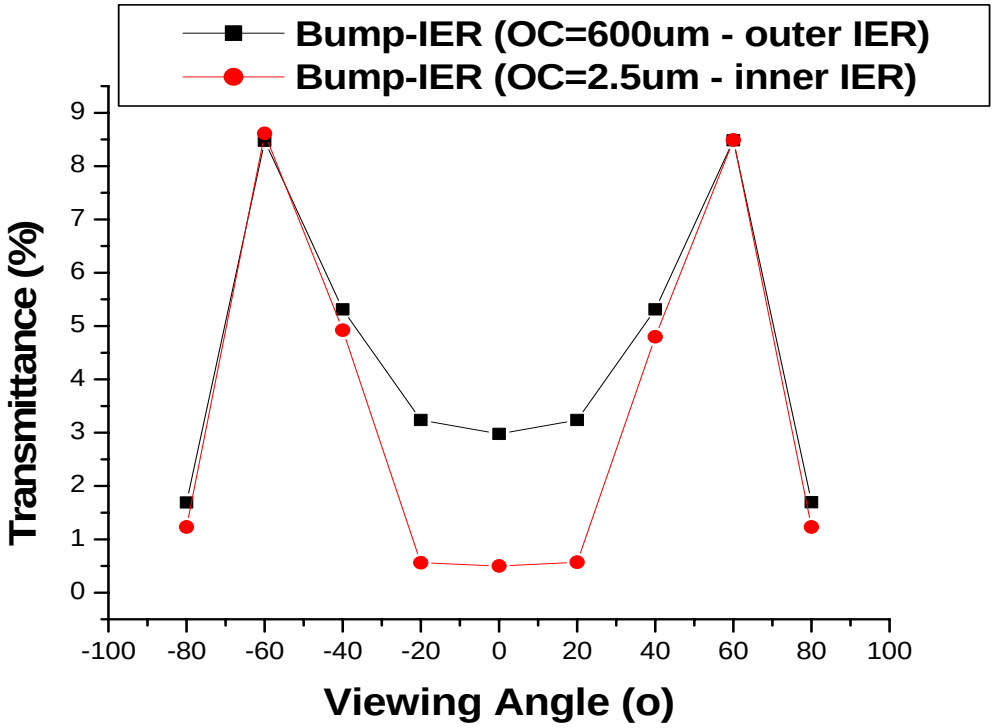

Fig.5.17 Measured light distribution at various OC thickness in transmissive mode with commercial backlight

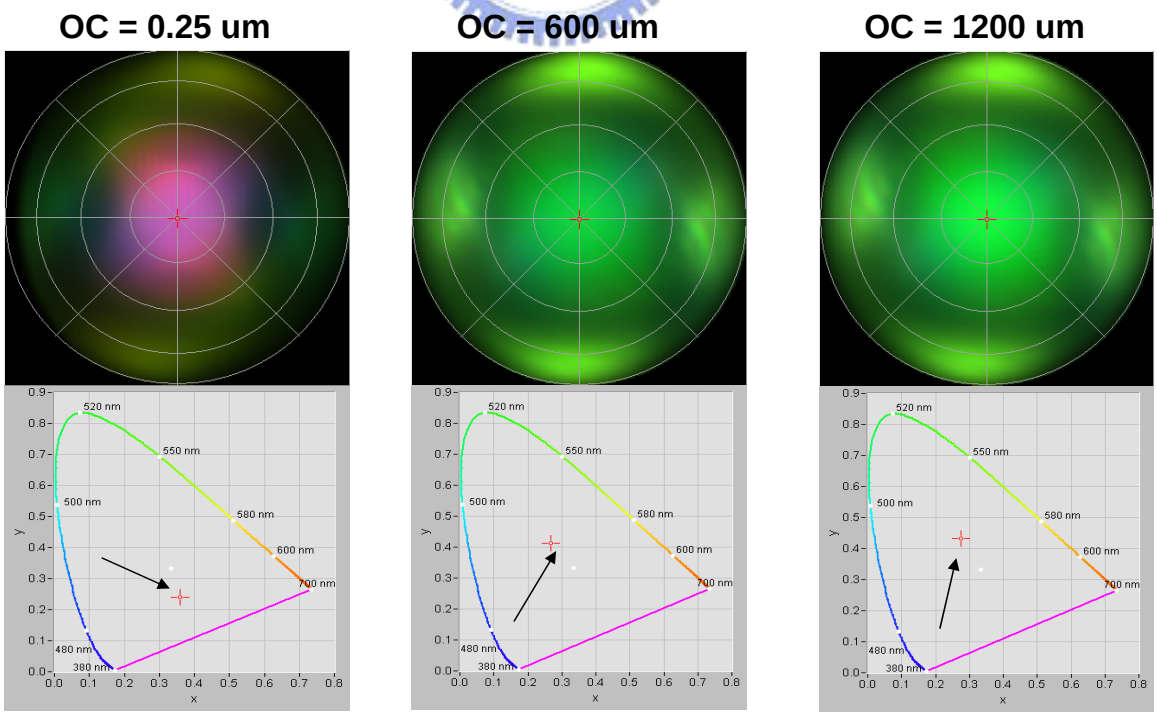

Fig. 5.18 Colorimetric evaluation at various OC thicknesses in the transmissive mode

In the reflective mode, the peak light was distributed at the normal incidence. As the OC thickness was increased, the luminance at the normal angle was decreased from 102 nits to 73 nits, yet the light distribution was essentially distributed at the normal angle when increasing the OC thickness, as shown in Fig. 5.20.

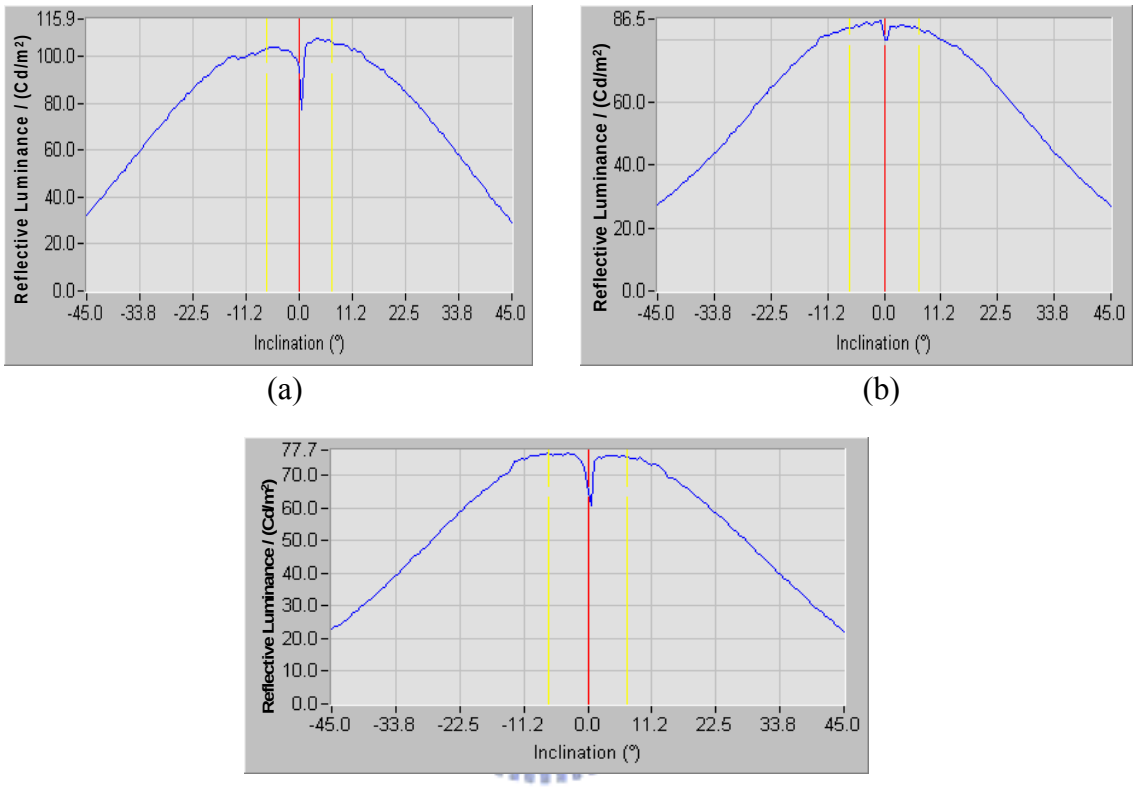

Fig.5.19 Measured light distribution at OC thickness of (a) 2.5μm (b) 150μm and (c) 600μm in reflective mode

5.3.3 Spectrum

Shown in Fig. 5.20 were the transmission and reflection spectrum of the translfective Ch-LCD in both bright and dark states. The cholesteric LC material with the reflection wavelength of 550 nm was utilized. In the bright states, the peak transmittance as well as reflectance of the device occurred was at the wavelength of λ=570 nm. Thus, with difference of light efficiency, the reflective modes demonstrated the light green color in the bright state, whereas the transmissive modes demonstrated the dark green color. Further, in the dark state, the reflectance of the

device was closed to 0.5% in the visible spectrum, whereas the transmittance has its peak value of 1.8% at the wavelength of 450nm. Thus, in the dark state the reflective mode demonstrated a black color whereas the transmissive mode displayed the bluish black. In summary, based on this results, the translfecitve Ch-LCD was able to display the same image color in any ambience.

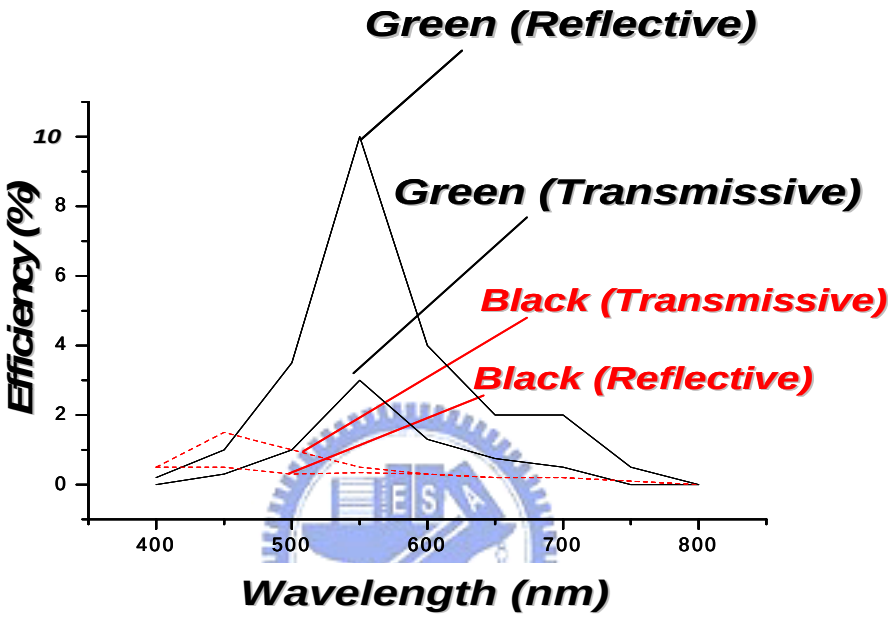

Fig. 5.20 Spectrum of the transflective Ch-LCD with outer IER structures

5.3.4 Comparison of Flat-shaped IER with bump-shaped IER

In the previous section, many optical evaluation including luminance, contrast ratio, and spectrum in both reflective and transmissive modes of transflective Ch-LCD were performed. In this section, the optical performances of the bump-shaped IER with the flat-shaped IER in transmissive mode will be compared. The OC thickness of 600μm was selected. The bottom substrate with hard-cured polyimide was then rubbed to produce the alignment characteristic of liquid crystal molecules. Finally, the reference backlight of 16255 nits was provided.

With the outer IER process, we have demonstrated that the split of the Al on the top of bump-IER was resolved and the tilt angle of bump-IER was reduced from 30˚

to nearly 15˚ in the pervious section. Thus, the fabricated results closely agreed with the desired design. However, contrary to our prediction, the results revealed that the peak transmittance for both bump-and flat-IER was still distributed at the ±60˚. The transmittance at the normal angle for both flat-and bump-shaped IER was still lower than 4%, yet the transmittance at ±60˚ of 8.8% was achieved. Therefore, based on the results, the transmittance of Ch-LCD was not considerably affected by the tilt angle.

The transmittance as well as reflectance of Flat-IER was shown in Fig. 5.24(a) and (b). The flat-shaped IER exhibited a superior performance than that of the bump-shaped IER. Compared to the bump-IER structure, the reflectance was increased from 6.1 % to 6.6 % and transmittance increased from 3 to 3.5% when the flat-shaped IER was utilized. These results suggest that the reflectance and transmittance were slightly enhanced when the Flat-IER was applied. Thus, the flat-shaped IER exhibited a superior reflectance and transmittance than that of the bump-shaped IER but with simpler fabrication process. Based on the results, the flat-IER has the advantages of simple fabrication, compatible to TFT process-Line as well as slightly superior performance, compared to bump IER. Thus, the flat-IER can be selected for fabricating IER film.

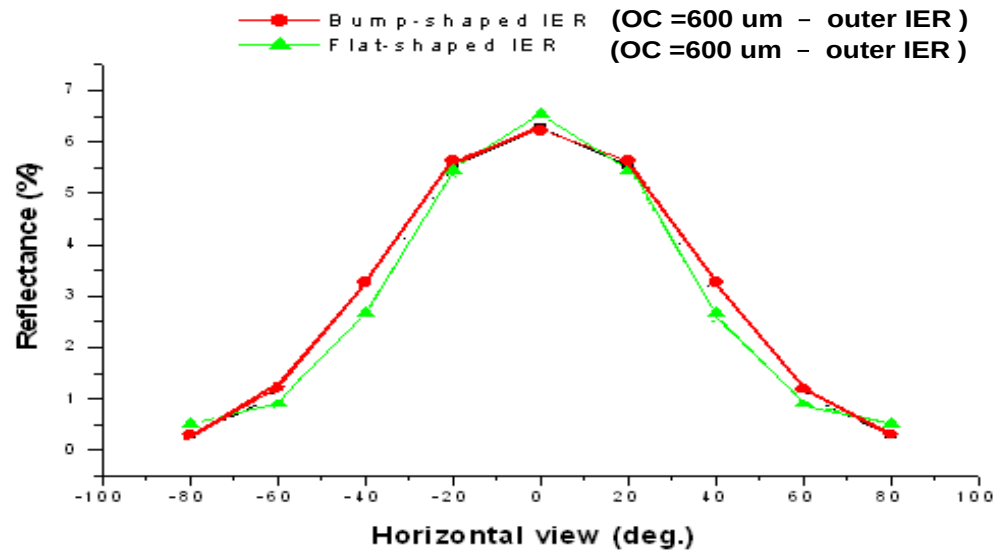

(a)

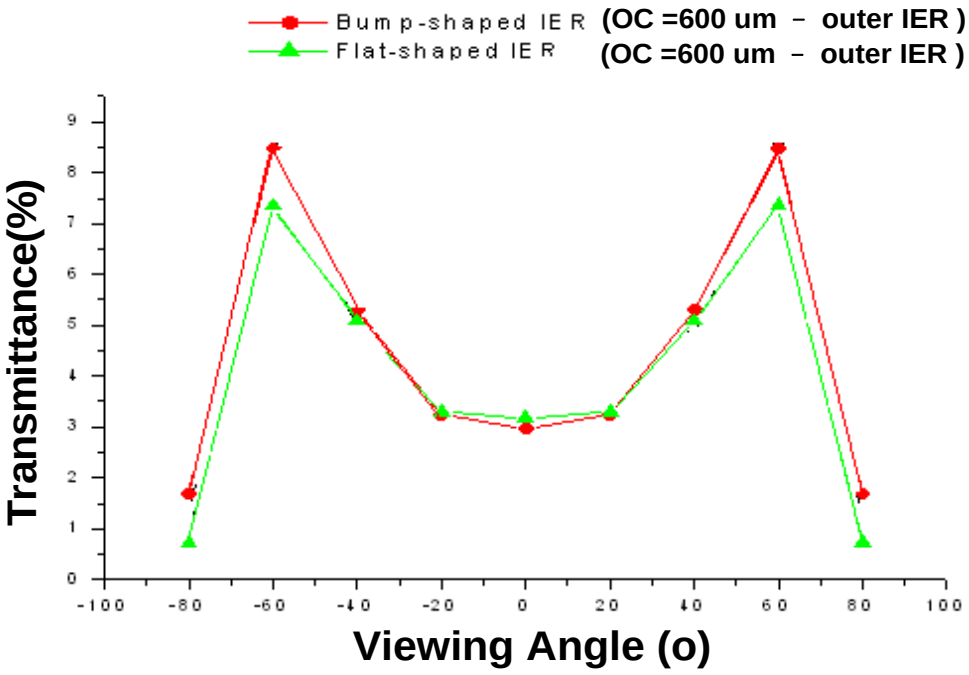

(b)

Fig. 5.21 (a) Reflectance and (b) transmittance of the transflective Ch-LCD using flat-shaped IER

5.3.6 Discussions

Tab. 5.6 was the comparison between the proposed transflective Ch-LCD with some company's reflective Ch-LCD.

Tab. 5.6 the comparison between the proposed transflective Ch-LCD with CPT's reflective Ch-LCD.

	Item	Transflective Ch-LCD (with IER film)	CPT's Reflective Ch-LCD
Transmissive mode	Transmittance	3.5%	None
	CR	5:1	None
	Viewing angle	-50˚~50˚	None
Reflective mode	Reflectance	7 %	26 %
	CR	5.5:1	4:1
	Viewing angle	-80˚~80˚	-70˚~70˚

From the measured results, both bright and dark states in the transmissive and reflective modes were obtained. The reflectance of 7 % was achieved as compared to the CPT's product of 26 %, whereas the transmittance of our transflective Ch-LCD was only 3.5 %. The CR of our proposed device performed superior than that of CPT's reflective Ch-LCD. Further, we found that the transmittance and reflectance were low compared to the conventional reflective Ch-LCD. The possible explanations resulting the differences between simulated and measured results were concluded as follows:

(a) **Unmatched index between each material:** As we mentioned that the IER can be extended to laminate on the upper substrate of Ch-LCD, the index matching issue needs to be concerned. To solve this issue, index-matched glue should be utilized between IER and the upper glass. As expected, the transmittance light efficiency will increase as less light will propagate into large viewing angle at the unmatched-index interface.

(b) **Insufficient rubbing conditions:** In this experiment, the rubbing condition was applied only to the bottom substrates. For the future experiment, more rubbing

condition should be applied for the optical performance comparison.

(c) Cross polarizer structure: the cross polarizer structure was obviously the main reason leading to the low reflectance and transmittance. Another method to solve the light leakage is by patterning the black matrix or absorption layer on the bottom substrate and then aligned with the IER / EIER structures. The transmittance and reflectance are expected to be improved by pattering the black matrix on the bottom substrate.

5.4 Visual Appearance

The actual display is made with the transflective mode. The device has two circular opposite polarity polarizers and IER / IER films. One polarizer with an opposite polarity to Ch-LC is laminated on the bottom substrate, whereas the same polarity polarizer is glued on the upper side of IER / EIER film. Afterward, simply implementing the IER / EIER film on to the upper substrate of Ch-LCD, the transflective Ch-LCD was realized as shown in the Fig. 5. 22. The photograph demonstrated that both transmissive and reflective modes display the same image color under any ambience, thus greatly improve the image quality of the transflective Ch-LCD.

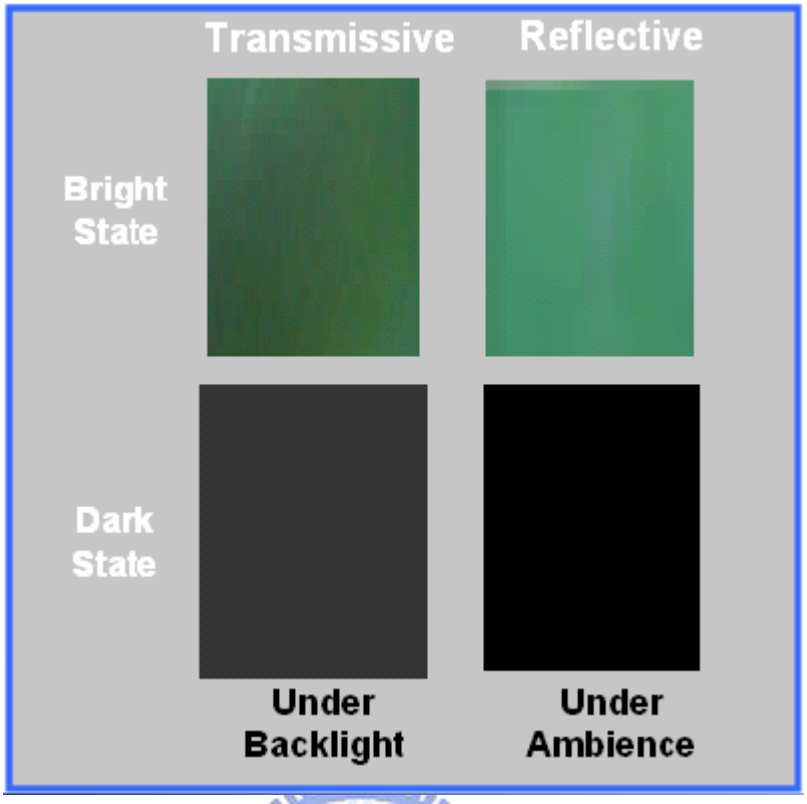

Fig. 5.22 Photograph of transflective Ch-LCD in transmissive mode under backlighting in a dark room and in reflective mode under office lighting.

5.5 Summary

In the section, the optical performances in both reflective and transmissive modes of the transflective Ch-LCD were evaluated. We also compared the measured results with the simulated results as well as CPT's commercial products. The results showed that at IER width of 14 μ m performed the highest reflectance and transmittance, as compared to the simulated results of 16 μ m. Further, EIER was proved to enhance the luminance and CR in transmissive mode, but degrade the performance in the reflective mode. Besides, the results revealed that the light distribution was mainly determined by the OC thickness. The IER was originally designed internally in the device laminated with the OC = 2.5μm. The results reveled that the transmittance was increased from 0.5 % to 3% as increasing OC = 2.5μm to 600μm, which is equivalent to the thickness of standard TFT glass substrate. Thus,

IER film was realized which can be laminated on the top of Ch-LCD, facilitating the fabrication process. The spectrum also demonstrated the bright state and dark state in both reflective and transmissive modes display the same image color, thus color transflective Ch-LCD can be realized by simply implementing our proposed structure into the well-developed color Ch-LCD such as color-stack device, without displaying complementary color.

Further, the flat-shaped IER exhibited a superior performance than that of the bump-shaped IER. Compared to the bump-IER structure, the reflectance was increased from 6.1 % to 6.6 % and transmittance increased from 3 to 3.5% when the flat-shaped IER was utilized. These results suggest that the reflectance and transmittance were slightly enhanced when the Flat-IER was applied and the IER film can be fabricated with only one mask, thus to reduce the fabrication cost and simplify the process as well as suitable to the TFT-process line.

However, the transmittance of 3-3.5 % and reflectance of 6-6.5% was insufficient to display the good image. Hence some possible solutions to enhance the normalized light distribution were proposed. First, we suggested that the black matrix should be applied on the bottom substrate with accurate alignment to the IER film to replace the current cross polarizer structure. With the black matrix method, the efficiency of both modes can be improved as well as the dark state can be obtained. Further, to focus the light distribution from large viewing angle to the normal direction the index-matched glue should be applied between the IER film and the Ch-LCD.

Chapter 6
Conclusions

6.1 Conclusion

A novel transflective liquid crystal display is demonstrated by using cholesteric liquid crystal as an LC layer and an image-enhanced reflector (IER) on the top of the transmissive sub-pixel, providing the similar paths for both reflected and transmitted light, and two circular polarizers laminated on the upper and rear substrates. An extended IER (EIER) is applied to enhance the brightness and CR. As a result, Ch-LCD displays the same image color in any ambience, thus greatly improve the image quality of the transflective cholesteric LCD.

The IER/EIER were built on the side of the pixel, thus to obtain nearly 100 % aperture ratio. Based on Bragg reflection of cholesteric LC in the planar texture, with the IER/EIER as well as functions circular polarizers, the bright states of both transmissive and reflective modes were obtained. Moreover, based on the scattering effect of cholesteric LC in the focal conic texture, the dark state was obtained with the IER/EIER as well as functions circular polarizers in both transmissive and reflective modes. Thus, a novel transflective Ch-LCD was realized by using cholesteric liquid crystal as a LC layer and IER/EIER on the top of the transmissive sub-pixel, providing the similar paths for both reflected and transmitted light, and two circular polarizers laminated on the upper and rear substrates. As a result, the proposed transflective Ch-LCD's were applicable to both monochromatic and full-color devices with same image color in any ambience.

In the simulation, we successfully designed and optimized the IER/EIER structures including IER/EIER widths and spacing between the IER/EIER and

cholesteric layer for high transmissive light efficiency. The transmissive light efficiency can be traded-off by increasing the IER width for reflective light utilization efficiency. Eventually, the optimized R:T ratio of 4:1 for the proposed transflective Ch-LCD is obtained by selecting IER and EIER width of 16μm and 5μm, respectively, in a pixel size of 210 x 210μm. The simulated overcoat results also demonstrated an essential application of the IER/EIER structures. The glass can be regarded as an overcoated layer, and thus the fabricated IER/EIER structure by the upper substrate process can be simply laminated on the conventional Ch-LCD.

In the fabrication process two fabricated results from the inner IER and outer IER process will be demonstrated. For the inner IER process, the IER was initially designed to fabricate inside the device, therefore, ITO was required for forming the electrode. For the outer IER process, the IER was extended to fabricate outside the device, thus in this process ITO was not required but the passivation layer was deposited.

The optical performances in both reflective and transmissive modes of the transflective Ch-LCD fabricated in both inner and outer IER process were evaluated as well as compared with the simulated results and CPT's commercial products. The results showed IER of 14μm performed highest reflectance as well as transmittance, as compared to simulated results of 16μm. EIER was proved to enhance the luminance and CR in transmissive mode, but reflectance was reduced as increasing the EIER width. Besides, the light distribution was mainly determined by the OC thickness in both reflective and transmissive modes. At OC = 600μm, equivalent to the thickness of standard TFT glass substrate, the transmittance of 2.6% was obtained as compared to 0.5% at OC = 2.5μm, where the IER / EIER were constructed in the cell. Thus, IER / EIER film was realized which can be laminated on any kinds of Ch-LCD, and with the function of opposite polarity polarizers, the transflective

Ch-LCD is obtained. Thus, for the future work, the full color transflective Ch-LCD could obtain by fabricated the color filter on the top of IER and utilized the high birefringence cholesteric material as a layer. Moreover, the transmittance of 3% was improved to 3.5% when the IER was fabricated with the flat-IER process, in which the flat-shaped was demonstrated and verified that it has the better performance than bump-shaped IER, in terms of reflectance and transmittance; hence flat-shaped can be the next IER candidate for easy fabrication process and compatible to the TFT-fabrication process. However, the low light efficiency in both modes needed to be improved, thus the bottom substrate is needed to be patterned by the black matrix to improve the efficiency. Further, the index-matched glue should be applied between the IER film and the Ch-LCD, to focus the light distribution at the normal angle.

In conclusion, the IER film was developed enabling the reflective Ch-LCD to upgrade into transflective Ch-LCD with the same image color under any ambience and hence enhancing the legibility in any ambience. We also discover that the flat IER perform superior than bump IER, thus facilitate the IER fabrication process.

Chapter 7
Future Work

7.1 Novel Full Color Transflective Ch-LCD by Inkjet Printing Method

The ink-jet printing (IJP) is a popular technology for desktop publishing and currently became an ideal method for print OTFT/PLED with high resolution since IJP is characteristics of patterning capability, large device area capability, efficiency of using material, and multicolor display fabrication capability. Moreover, it is well known that the cholesteric texture has the advantages of displaying the spectrum ranging from inferred, to visible and even to ultraviolet band, thus Ch-LC material performs outstanding achievement in the aspect of displaying full color capability. To achieve the full color Ch-LCD display, we proposed the first work of using the piezoelectric IJP[19] to deposit the patterned RGB Ch-LC materials droplets on the corresponding reflective region of sub-pixel on the bottom substrate.

Our objective is to demonstrate that the Ch-LC with extremely high viscosity is compatible with IJP and the Ch-LC droplet with high stability can be deposited on the glass substrate. We first try with green Ch-LC for initial testing. FM-M01 Ch-LC (central wavelength= 550nm, green light band) provided by MERK was utilized for deposition. The printing system was developed by ITRI. The SE-128 piezoelectric printhead provided by Spectra was utilized in this printing system. For obtaining the uniform droplet with the Spectra's printhead, the viscosity of ink material should be ranging from 1~15 cps to obtain high stable printing. Since the viscosity of Ch-LC was extremely high, thus decreasing the viscosity to 10 cps was the key technique to deposit the cholesteric droplet. As shown in Fig. 12, the viscosity of the cholesteric material was dropped to 10 cps when we increased the temperature to 60˚C. As a

result, the printhead started to squeeze the green cholesteric droplet as shown in Fig. 13. The flying motion image of the droplet was begun at 10μs and was snapped shot at the time interval of 15μs. From this figure, we see that each snap shot at corresponding interval demonstrated a sharp edge around the droplet. Thus, we can conclude each droplet was demonstrated with high stability and the Ch-LC material is highly compatible with the Spectra printing head.

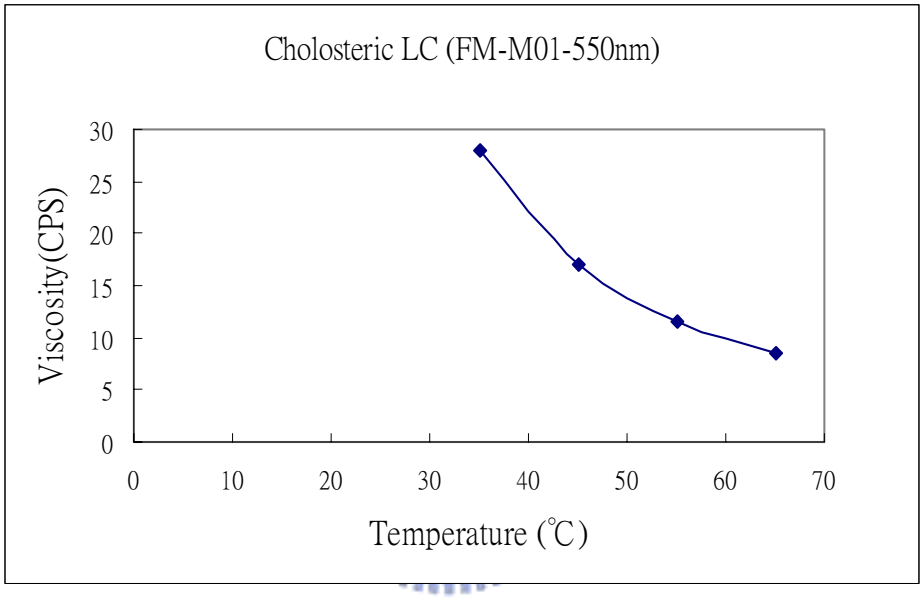

Fig. 7.1 Relationship between temperature and viscosity of Ch-LC using piezoelectric IJP

As a result, we successfully deposited dot-patterned Ch-LC on the glass substrate, as shown in Fig. 14. The dot diameter was 120μm and lateral and vertical pitches were 300μm and 508μm, respectively. From the figure the satellite dot was very few, and thus the stability to deposit the dot Ch-LC was high. Further, by continuous depositing the dot Ch-LC, we successfully deposit the stripe-patterned Ch-LC on the glass substrate, as shown in Fig. 15. The diameter was still 120μm and the vertical pitch was 508μm. From the figure, only a small number of satellite dots were appeared near the stripe Ch-LC. Thus, the stability to deposit the Ch-LC with the Spectra printhead was high. As the dot- and stripe-patterned Ch-LC with high printing

quality were obtained, various patterning types can be achieved by modifying the computer program to inject the Ch-LC ink in-between the banks or walls with particular patterns, such as mosaic and stripe types.

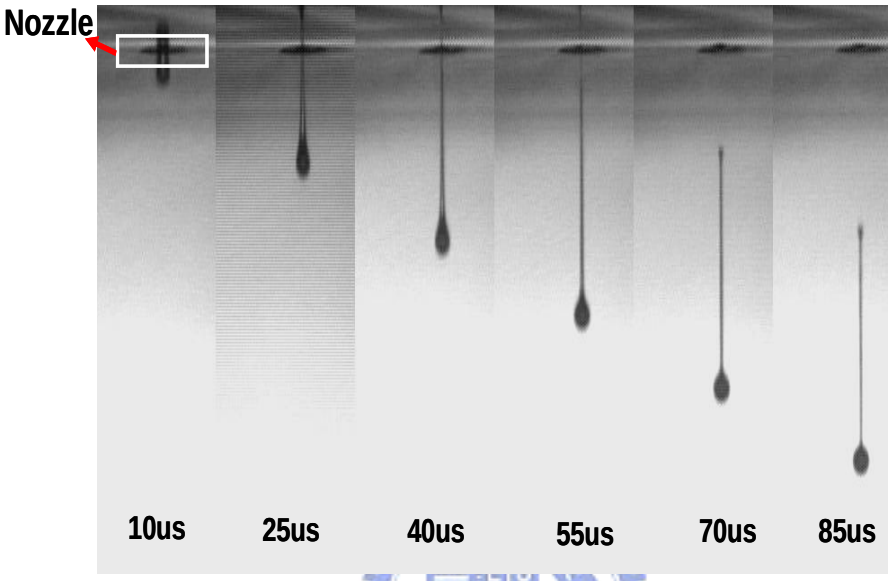

Fig. 7.2 Flying motion of printing Ch-LC droplet by snapping shot at time interval of 15μs.

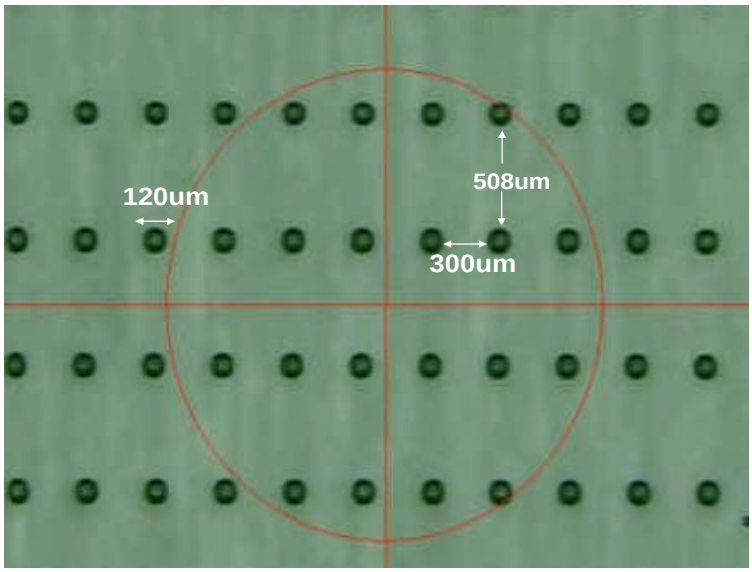

Fig. 7.3 Cholesteric LC's dot pattern deposited on the glass substrate by IJP

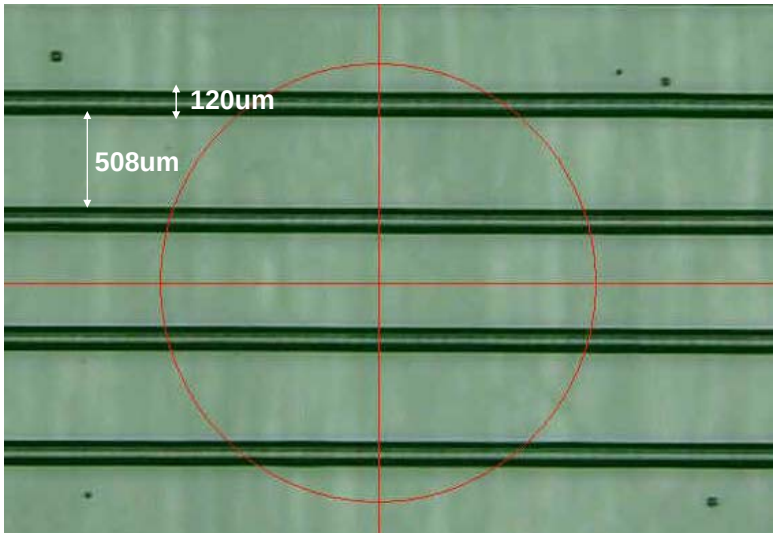

Fig. 7.4 Cholesteric LC's stripe pattern deposited on the glass substrate by IJP

7.2 Future Work

Since the initial injection with green Ch-LC was successfully demonstrated, thus the RGB Ch-LC will be deposited on reflective region patterned with black matrix on the bottom substrate. Then IER film will be position in the transmissive region patterned with high transmittance wall on the bottom substrate. As a result, the full color Ch-display will be obtained, as shown in Fig. 16. Further, IJP technique with Ch-LC can also be used in the color filter application with characteristics of high efficiency. Since Ch-LC is able to display full color capability and was polarizerless (Bragg Reflection), thus, with IJP (no mask is required), 100% reflection can be easily achieved by pattering the left-handed RGB Ch-LC and right-handed RGB Ch-LC[9]. With the benefits of IJP, the RGB pattern were obtained without using the conventional semiconductor process requiring additional mask charge. Further, according to the simulation results on OC thickness, the optimized transmittance of 14% was obtained at OC thickness ranging from 150~200μm. Thus, to obtain high transmittance with this specific OC thickness, the plastic substrates as an OC layer should be applied. Therefore, the flexible transflective Ch-LCD can be realized with

the plastic IER film on the plastic substrates, and to obtain with full-color capability, the IJP with cholesteric ink will be further applied on the plastic substrates.

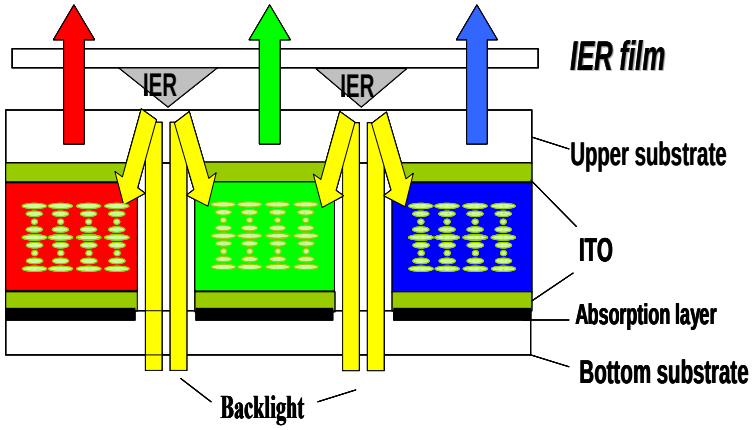

Fig.7.5 Full color transflecitve Ch-LCD with IER film and IJP method

Reference

[1] X. Y. Huang, Kent Displays, IDW'01, P.465,

[2] T. Uchida, SID 1996, 31.

[3] J.A.M.M. van Haaren, C. Doornkamp, H.J. Cornelissen,, L.J.M. Schlangen, J.P.A. Deeben, P. van de Witte, R van Asselt, IDW 1999, 331

[4] D.-K. Yang, J. L. West, L.-C. Chien, J. W. Doane, J. Appl.Phys., 76 20 (July 1994).

[6] A. Tanaka, SID Intl. Symp. Digest Tech. Papers, 33 1240 (2002)

[7] Rob van Asselt1, Rob A.W. van Rooij1, Dirk J. Broer, SID'02, p.742

[8] Y. P. Huang, M. J. Su, H. P. D. Shieh, and S. T. Wu, Proc. SID'03, p. 86 (2003).

[9] S. Chandrasekhar, Liquid crystals, 2nd ed., Cambridge University Press, New York, (1997)

[10] D. K. Yang, J. L. West, L. C. Chien, and J. W. Doane, J. Appl. Phys. 76, p. 1331 (1994)

[11] P. G. De Gennes, and J. Prost, The physics of liquid crystals, Oxford University Press, New York (1993).

[12] Z. J. Lu, W. D. St. John, X. Y. Huang, D. K. Yang, and J. W. Doane, Proc. SID'95, p.172 (1995)

[13] X. Y. Huang, N. Miller, A. Khan, D. Davis, and J. W. Doane, Proc. SID'98, p.810 (1998)

[14] M, Xu, and D. K. Yang, Optical properties of the gray-scale states of cholesteric reflective displays, Proc. SID'99, p. 950 (1999)

[15] D. Davis, A. Khan, C. Jones, X. Y. Huang, and J. W. Doane, J. SID 7, p. 43 (1999).

[16] D. Davis, K. Khan, X. Y. Huang, and J. W. Doane, Proc. SID'98, p.901 (1998).

[17] M. Born, and E. Wolf, Principle of Optics, Pergamon Press, New York, (1998).

[18] S. Martellucci, and A. N. Chester, Diffractive Optics and Optica Microsystems, Plenum, New York (1997).

[19] M. Grove, D.Hayes, R.Cox, D.Wallace, “Color Flat Panel Manufacturing Using Ink Jet Technology”, Display Works(1999), p1